arXiv:hep-lat/9309015v1 23 Sep 1993

September 1993 UCSD/PTH 93-28, Wash. U. HEP/93-60
hep-lat 9309015

Investigation of the domain wall fermion approach to chiral gauge theories on the lattice

Maarten F.L. Golterman[a,1], Karl Jansen[b,2], Donald N. Petcher[a,3]
and Jeroen C. Vink[b,4]

[a]Washington University, Deparment of Physics, St. Louis, MO 63130, USA
[b]University of California at San Diego, Department of Physics 0319,
La Jolla, CA 92093, USA

Abstract
We investigate a recent proposal to construct chiral gauge theories on the lattice using domain wall fermions. We restrict ourselves to the finite volume case, in which two domain walls are present, with modes of opposite chirality on each of them. We couple the chiral fermions on only one of the domain walls to a gauge field. In order to preserve gauge invariance, we have to add a scalar field, which gives rise to additional light mirror fermion and scalar modes. We argue that in an anomaly free model these extra modes would decouple if our model possesses a so-called strong coupling symmetric phase. However, our numerical results indicate that such a phase most probably does not exist.

[1]e-mail: maarten@wuphys.wustl.edu
[2]e-mail: jansen@higgs.ucsd.edu,
Address after October 1: DESY, Notkestrasse 85, 22603 Hamburg 52, Germany
[3]e-mail: petcher@moriah.covenant.edu,
present address: Dept. of Phys., Covenant College, Lookout Mountain, GA 30750, USA
[4]e-mail: vink@yukawa.ucsd.edu

1 Introduction

The lattice provides a first-principles regularization of quantum field theories, which allows us to explore the nonperturbative properties of a model and for vectorlike theories, such as QCD, it has proven to be very successful. Since the full Standard Model is a chiral gauge theory, it is natural to attempt a construction of chiral gauge models on the lattice as well.

As is well known, however, on the lattice one is confronted with "species doubling" [1, 2], i.e. the phenomenon that a single Weyl fermion field on the lattice leads to an equal number of left and right handed fermions in the continuum limit. When coupled to a gauge field, all doublers transform in the same representation of the gauge group which prevents an easy construction of chiral gauge theories. For nonchiral models there are two well tested ways of dealing with the species doublers: they can be decoupled with a momentum dependent mass term as in Wilson's method, or they can be used as physical degrees of freedom as in the staggered fermion method. However, since these methods violate chiral symmetry, a straightforward extension to chiral gauge theories would clash with gauge invariance. Proposals for chiral gauge theories on the lattice include generalizations of Wilson's method [3–6] and of the staggered method [7]. There are proposals that try to avoid coupling the doublers [8], and approaches that start from a gauge-fixed continuum action [9, 10]. There are also proposals for more radical departures from the usual lattice fermion prescriptions [11–13]. For a recent review, see ref. [14].

The domain wall fermion approach suggested in ref. [12] falls into the last group and has attracted a lot of attention recently [15–22]. In the domain wall model an extra dimension is added to our four dimensional world. In this five dimensional world the model is vectorlike and the fermion doublers can be removed using Wilson's method without breaking gauge invariance. The reduction to a four dimensional world with a chiral fermion is made by giving the fermions a mass term which flips sign across a four dimensional domain wall. It has been shown [12] that the lattice Wilson-Dirac operator with such a mass term has a chiral zeromode, which is bound to the domain wall. This fermion remains massless and localized at the domain wall for (four-)momenta below a critical momentum [12, 15, 17]. On a finite lattice the (periodic) boundary conditions lead to a second anti-domain wall with a chiral fermion of opposite handedness.

Every lattice model for a chiral gauge theory has to produce the appropriate anomaly structure of the target continuum theory. The domain wall model has the potential to solve this problem elegantly with the help of the extra dimension. The starting five dimensional model is vectorlike and hence the gauge current J_μ is anomaly free, $\sum_{\mu=1}^{5} \partial_\mu J_\mu = 0$. However, the four dimensional current restricted to the domain wall is clearly not conserved $\sum_{\mu=1}^{4} \partial_\mu J_\mu = -\partial_5 J_5$, and its divergence reproduces the expected anomaly when computed for weak external gauge fields [12, 15, 18]. J_5 takes the form of a Goldstone-Wilczek current with a nonzero derivative across the domain wall, as

was demonstrated some time ago in the continuum in ref. [23]. On a finite lattice this Goldstone-Wilczek current transports charge from the domain wall to the anti-domain wall, ensuring charge conservation in the five dimensional theory. The same mechanism should also yield the correct four dimensional global anomaly structure.

In the work referred to above the domain wall fermions are coupled to fixed smooth external gauge fields. Here it is not important that the chiral fermions at both the domain and anti-domain walls couple to the gauge field, because we can single out one of the domain walls by hand. With dynamical gauge fields, however, the crucial requirement is that only a single domain wall fermion couples to the gauge field. If this can be achieved the second domain wall can be ignored and we are left with an interacting chiral fermion in a four dimensional world located at the domain wall, assuming that the fermions are in an anomaly free representation.

In the original proposal it was hoped that the communication between the two domain walls could be prevented by modifying the gauge interactions in the fifth dimension. However, it seems likely that this approach does not lead to the desired decoupling (see also ref. [22]) and here we follow instead the suggestion made in ref. [24]. In this approach the gauge fields are coupled only in a restricted region around one of the domain walls, where the size of this region, which we will call the waveguide, should be at least as large as the support of the wave function of the domain wall zeromode. However, as will be discussed in much more detail below, the requirement of gauge invariance leads to the introduction of an extra scalar field at the boundaries of the waveguide. This scalar field screens the gauge charge of the fermions at the waveguide boundary and allows for interactions between these charged fermions and the neutral ones outside the waveguide. This leads to Yukawa couplings located at the waveguide boundary which give rise to additional light fermion modes at the waveguide boundary. This is most easily seen for zero Yukawa coupling, because then the waveguide region decouples from the anti-domain wall region and five dimensional charge conservation is now ensured by the new zeromodes at the boundary.

The aim is then to decouple the fermion at the waveguide boundary and maintain at the same time the chiral zeromode at the domain wall. Because we have introduced a scalar field coupled to the fermions through a Yukawa interaction, we may hope for a rich phase structure of the model, similar to that found in other two and four dimensional Yukawa models on the lattice. In particular, one expects that one can drive the system into a symmetric phase, with vanishing scalar field vacuum expectation value v, and a spontaneously broken phase, with $v > 0$. For small values of the Yukawa coupling one then expects the fermions at the waveguide to follow the perturbative relation $m_F \propto v$ (with $v = 0$ in the symmetric phase). This means that these fermions remain light and appear in the low energy spectrum. However, at large values of the Yukawa coupling, the interaction of the fermion and scalar fields might become so strong that only a bound state fermion exists with a mass of the order of the cutoff. Such a strong coupling behavior has been established in various Yukawa models on the lattice [25–27]. If the

four dimensional model is anomaly free and if we choose the waveguide boundary with the scalar field far enough from the domain wall, we could hope to take the waveguide fermions into a strong coupling symmetric phase, without affecting the chiral mode at the domain wall. Then the fermions at the waveguide boundary would decouple from the low energy physics, leaving only the chiral zeromodes at the domain wall coupled to the gauge field.

The crucial question we will investigate in this paper is therefore whether such a strong symmetric phase exists in the domain wall model. We will present evidence based on analytical considerations and numerical results, which leads us to conclude that an appropriate strong coupling phase most probably does not occur.

The paper is organized as follows. In sect. 2 we review free domain wall fermions, discuss the coupling to the gauge field and the need to introduce the extra scalar field. We close the section with a sketch of the phase diagram we would hope to find for our model. In sect. 3 we rewrite the fermion action in a mirror-fermion form, such that we can distinguish the light modes from the heavy ones. In the next section we present results for fermion masses, concentrating on the results for the boundary fermion. In sect. 5 we continue our search for a strong coupling phase using the eigenvalue spectra of the fermion matrix in a simplified model, in which all heavy modes are discarded. Sect. 6 contains a brief discussion of alternative ways to couple the gauge field and in sect. 7 we present our conclusions.

2 Domain wall fermions coupled to gauge fields

2.1 Resumé of free domain wall fermions

Let us start our discussion with a short resumé of free domain wall fermions. Consider an odd dimensional lattice of size $L^d L_s$, with $d = 2n$, L_s the extent in the extra dimension and lattice sites labeled by (x, s), $(x \equiv (x_1, \cdots, x_d))$. The action for free domain wall fermions [12] can be written as,

$$\begin{aligned} S_\Psi &= \sum_s \left(\sum_{xy} \overline{\Psi}^s_x (\partial\!\!\!/\,_{xy} - w_{xy} + m^s \delta_{x,y}) \Psi^s_y \right. \\ &- \left. \tfrac{1}{2} \sum_x [\overline{\Psi}^s_x (r - \gamma_5) \Psi^{s+1}_x + \overline{\Psi}^{s+1}_x (r + \gamma_5) \Psi^s_x - 2r \overline{\Psi}^s_x \Psi^s_x] \right), \end{aligned} \tag{2.1}$$

where $\partial\!\!\!/$ and w are the Dirac operator and Wilson term with Wilson parameter r on the even d dimensional lattice,

$$\partial\!\!\!/\,_{xy} = \sum_{\mu=1}^{d} \tfrac{1}{2} \gamma_\mu [\delta_{x+\hat{\mu},y} - \delta_{x-\hat{\mu},y}],$$

$$w_{xy} = \sum_{\mu=1}^{d} \tfrac{1}{2} r[\delta_{x+\hat{\mu},y} + \delta_{x-\hat{\mu},y} - 2\delta_{x,y}]. \tag{2.2}$$

The $\delta_{x,y}$ is the Kronecker delta and we use lattice units $a = 1$. We shall choose the Wilson parameter $r = 1$ for convenience and for the domain wall mass, denoted by m^s, we choose a periodic step function of the form (with L_s even),

$$\begin{aligned} m^s &= -m_0 \quad s = 2, \cdots, L_s/2, \\ m^s &= 0 \quad s = 1, L_s/2+1, \\ m^s &= +m_0 \quad s = L_s/2+2, \cdots, L_s. \end{aligned} \tag{2.3}$$

With periodic boundary conditions in s, the emergence of an anti-domain wall is inevitable. It will often be convenient to think of s as a flavor label, rather than an extra space-time coordinate.

This model posesses two chiral zeromodes with the property that the mode bound to the domain wall at $s = 1$ is left handed ($\gamma_5 = -1$) and the mode bound to the other domain wall at $s = L_s/2+1$ is right handed ($\gamma_5 = +1$) [12]. The wave functions for both modes have the form of plane waves in the $2n$-dimensional space and decay exponentially in s, away from the domain walls. These chiral zeromodes exist for plane wave momenta below some critical momentum p_c which depends on the ratio m_0/r. For different values of m_0/r the zeromode spectrum can change substantially. For $0 < m_0/r < 2$ one has only one chiral zeromode at each domain wall. For increasing values of m_0/r this zeromode becomes less localized and disappears at $m_0/r = 2$. At this point new zeromodes with opposite chirality are provided by the species doublers which are located at different corners of the Brillouin zone [17, 18]. Throughout the paper we will take $m_0/r \approx 1$ and hence we will have only one chiral zeromode at the domain wall with exponentially small overlap with the zeromode at the anti-domain wall. In this case, chiral modes exist for momenta p below a critical momentum, $|\hat{p}| < p_c$, with $\hat{p}^2 = 2\sum_\mu (1 - \cos(p_\mu))$ and $p_c^2 = 4 - 2m_0/r$. Note that $\hat{p}^2 \approx p^2$ for small momenta.

2.2 Coupling to gauge fields

Since the left and right handed zeromode components of the fermion field now are separated in s space, one can attempt to couple these two components in different ways to a gauge field. If we succeed in coupling only one of the two zeromodes to a gauge field, we can hope to use this in order to construct a chiral gauge theory on the lattice. This appears to be impossible if one also insists that gauge invariance is maintained. However, if we do not worry about gauge invariance for the moment, we can couple the right handed mode to a gauge field, by replacing the free ($2n$-dimensional) Dirac operator and Wilson term by the gauge invariant ones, but only for a restricted number of s-slices around the right-handed domain wall, cf. [24]. In this way the gauge field

is confined within a "waveguide" around the domain wall, and interactions with the opposite chirality mode at the anti-domain wall are exponentially suppressed with L_s.

We take the same gauge field on all s-slices inside the waveguide, which is natural if one thinks of s as a flavor label, and define gauge transformations on the fermion field as

$$\begin{array}{rclcrcll} \Psi_x^s & \to & g_x \Psi_x^s, & & \overline{\Psi}_x^s & \to & \overline{\Psi}_x^s g_x^\dagger & s \in WG, \\ \Psi_x^s & \to & \Psi_x^s, & & \overline{\Psi}_x^s & \to & \overline{\Psi}_x^s & s \notin WG, \end{array} \tag{2.4}$$

$$WG = \{s : s_0 \le s \le s_0'\} \tag{2.5}$$

with g_x in a gauge group G. The detailed choice of the boundaries s_0 and s_0' is not very important, provided they are sufficiently far from the domain wall that the zeromode is exponentially small at the waveguide boundary. For symmetry reasons we shall choose $s_0 = (L_s+2)/4+1$ and $s_0' = (3L_s+2)/4$, such that the right handed mode at $s = L_s/2+1$ is located at the center of the waveguide, see fig. 1. With this choice we have to take $L_s - 2$ a multiple of four.

Having made this division into a waveguide and its exterior, we note that the model has a global $G \times G$ symmetry:

$$\begin{array}{rclcrcll} \Psi_x^s & \to & g \Psi_x^s, & & \overline{\Psi}_x^s & \to & \overline{\Psi}_x^s g^\dagger, & s \in WG, \\ \Psi_x^s & \to & h \Psi_x^s, & & \overline{\Psi}_x^s & \to & \overline{\Psi}_x^s h^\dagger, & s \notin WG. \end{array} \tag{2.6}$$

With our choice for the position of the waveguide boundary, there is a symmetry involving parity plus a reflection in the s-direction with respect to the plane $s = s_0 - \frac{1}{2} = L_s/4 + 1$,

$$\Psi_x^s \to \gamma_d \Psi_{Px}^{L_s/2+2-s}, \tag{2.7}$$

with $Px = (-x_1, \cdots, -x_{d-1}, x_d)$ the parity transform of x.

It is clear that the hopping terms from $s_0 - 1$ to s_0 and from s_0' to $s_0' + 1$ break the local gauge invariance of eq. (2.4). However, this can be repaired by putting in a scalar field V at the boundary of the waveguide, or alternatively by interpreting the gauge field g_x that appears in the action after performing a gauge transformation as a Stückelberg field. This leads to the gauge invariant action

$$\begin{aligned} S_\Psi &= \sum_{s \in WG} \overline{\Psi}^s (\not{D}(U) - W(U) + m^s) \Psi^s + \sum_{s \notin WG} \overline{\Psi}^s (\not{\partial} - w + m^s) \Psi^s \\ &- \sum_{s \neq s_0 - 1, s_0'} [\overline{\Psi}^s P_L \Psi^{s+1} + \overline{\Psi}^{s+1} P_R \Psi^s] + \sum_s \overline{\Psi}^s \Psi^s \\ &- y(\overline{\Psi}^{s_0 - 1} V P_L \Psi^{s_0} + \overline{\Psi}^{s_0} V^\dagger P_R \Psi^{s_0 - 1}) - y(\overline{\Psi}^{s_0'} V^\dagger P_L \Psi^{s_0'+1} + \overline{\Psi}^{s_0'+1} V P_R \Psi^{s_0'}), \end{aligned} \tag{2.8}$$

where we have supplied the Yukawa term with a coupling constant y. Note that we take the same scalar field at both waveguide boundaries. Since we have chosen $r = 1$ we have written projectors in the hopping terms in s, $P_{R(L)} = \frac{1}{2}(1 + (-)\gamma_5)$. $\not{D}(U)$ and $W(U)$

are the usual gauge covariant Dirac operator and Wilson term, whose explicit form is not important here, since we shall only work with $U = 1$ in this paper. The field $V_x \in G$ is the scalar field, which can be thought of as a (radially frozen) Higgs field, and which transforms as

$$V_x \to h V_x g_x^\dagger. \tag{2.9}$$

The transformation given in eq. (2.7) remains a symmetry if V transforms as

$$V_x \to V_{Px}^\dagger. \tag{2.10}$$

Since gauge invariance is broken in the model without scalar field, we add a mass term for the gauge boson, which on the lattice takes the form $\kappa \sum_\mu \mathrm{tr}\,(U_\mu + U_\mu^\dagger)$, with κ the mass parameter in lattice units. It takes the form of a hopping term for V when this field is used to restore the gauge invariance of this mass term,

$$S_V = -\kappa \sum_{x,\mu} \mathrm{tr}\,(V_x U_{\mu x} V_{x+\hat{\mu}}^\dagger + h.c.). \tag{2.11}$$

Gauge invariance and the necessity to couple only the zeromode on one of the domain walls to the gauge field has led to an action which contains an additional scalar field. One might wonder whether there is a better way to introduce a gauge field which couples to only one of the domain wall zeromodes, but avoids the extra scalar field. Unfortunately, this appears to be difficult, if not impossible in a model which contains both domain walls, as we shall argue in sect. 6. For a proposal in a different direction, in which the anti-domain wall is avoided by keeping L_s strictly infinite, see ref. [20].

To get an idea about the physics of the model (2.8), we can start with $y = 0$, in which case the scalar field is decoupled. However, now the gauged and ungauged parts of the action have decoupled completely as well, which implies that the two zeromodes on the domain walls are no longer balanced by each other. Therefore new zeromodes with opposite chirality must emerge which will be bound to the waveguide boundary. As an illustration we have plotted in fig. 1 the four zeromodes computed for the smallest plane wave momentum on a lattice with $d = 2$, $L_s = 50$ and $U = 1$. At $y = 0$ (figure 1a) one recognizes the two expected massless modes at the domain walls, but also two modes at the waveguide boundary. These modes are massless[1], because there can be no overlap between the left and right handed components across the waveguide boundary. For nonzero y the two components can overlap and they form a Dirac state with mass approximately equal to y, see fig. 1b, where we took $V = 1$. One clearly sees how in this case the wave functions which are peaked at the waveguide boundary extend across this boundary. Note that the modes shown in fig. 1 are symmetric around the waveguide boundary, in accordance with the symmetry given in eq. (2.7). The extra mirror modes at the waveguide boundary will be further discussed in the next section.

[1]Of course, these modes are not exactly massless, because of the exponentially suppressed mixing between the domain wall and boundary modes.

2.3 Conjectured phase diagram

To arrive at a chiral model, both this additional fermion at the waveguide boundary and the scalar field have to be decoupled. We first make the simplification of neglecting the gauge field dynamics by replacing $U \to 1$. This is reasonable, because we are interested in the scaling region at small gauge coupling. There we can write $U_{\mu x} = \Omega_x U^L_{\mu x} \Omega^\dagger_{\mu x+\hat{\mu}}$ with U^L the gauge field in the smooth Landau gauge. The Ω can be absorbed by a gauge transformation on ψ, $\overline{\psi}$ and V. Since U^L is now smooth and close to one, we can treat this field in perturbation theory and put $U = 1$ in our numerical computations. Note that at large Yukawa couplings the scalar field dynamics cannot be computed in perturbation theory.

The light fermion modes are well localized, which implies that the mode at the domain wall has only an exponentially small overlap with the scalar field at the waveguide boundary. With $r = 1$ the domain wall zeromode has a magnitude $\propto e^{-m_0 L_s/4}$ at the waveguide boundary, and for sufficiently large L_s the effective Yukawa coupling to the scalar field is exponentially suppressed, $ye^{-m_0 L_s/4}$. The new fermion mode, on the other hand, is localized at the s-slice that carries the scalar field and is coupled to it with strength y. Therefore we can use the freedom of adjusting the coupling constants y and κ to try to decouple the unwanted fields at the waveguide boundary, while keeping L_s sufficiently large as to ensure that the physics of the zeromode at the domain wall will remain unaffected.

In the broken phase (or ferromagnetic (FM) phase), where the scalar field expectation value $v = \langle V_x \rangle$ is nonzero, we expect that the boundary fermion for small y gets a mass $\propto yv$, but also the gauge boson acquires a mass $\propto v$. Therefore we cannot decouple the fermion while keeping the gauge boson light. If we allow the gauge boson to be massive, it follows from the triviality of the Yukawa coupling in this region of the phase diagram, that the fermion mass will be of comparable magnitude. The remaining option is to choose κ in the symmetric phase (or paramagnetic (PM) phase). Here we expect from experience with the massive Yang-Mills model that the scalar field can be decoupled from the low energy physics of the fermion-gauge model, because deep inside the symmetric phase all scalar excitations will have masses of the order of the cutoff. However, since $v = 0$, one would also expect the boundary fermion to have mass zero and therefore not to decouple, which implies that the low energy model would be vectorlike.

An interesting possibility is however that our model might exhibit the strong Yukawa coupling behavior found in other lattice Higgs-Yukawa models [25–27]. It was shown that for strong Yukawa couplings in the symmetric phase, such models exhibit another phase (denoted by PMS) in which the fermion and the scalar field form a massive bound state with mass of the order of the cutoff. We illustrate this desirable scenario with a possible phase diagram at $\kappa = 0$ for our model, for the Yukawa couplings y and $ye^{-m_0 L_s/4}$ of the waveguide boundary and domain wall fermions respectively, shown in fig. 2.

For $L_s \to \infty$, the domain wall fermion has negligible Yukawa coupling, and we can

hope the phase diagram to be similar to that of the Yukawa model studied in ref. [27]: for small y the system starts off in a weak symmetric phase (PMW); for increasing y the system comes into a broken phase, because the induced fermion interactions are of ferromagnetic nature. Then for still larger y the system enters a strong symmetric phase in which the boundary fermion becomes massive (denoted by PMS_1).

For finite values of L_s also the domain wall fermion gets strongly coupled for large y and this could take the system into a different symmetric phase (denoted by PMS_2), in which both fermions are massive. Like between the PMW and PMS_1 phases, there may be a FM phase separating the PMS_1 from the PMS_2, cf. fig. 2. We note in passing that the presence of two Yukawa couplings which are both proportional to y but differ by a large factor $e^{m_0 L_s/4}$ makes it very difficult to apply a strong coupling expansion in y, to investigate or establish the PMS_1 phase analytically.

If the phase diagram of fig. 2 would be qualitatively correct for our model and a PMS_1 phase does exist, we could decouple the unwanted boundary fermion as well as the scalar field: we can choose the Yukawa coupling y sufficiently strong that the boundary fermion forms a bound state with the scalar field and acquires a mass of the order of the cutoff, whereas the domain wall fermion still is weakly coupled and remains massless. Sufficiently deep in this PMS_1 phase also the scalar field is very massive and should decouple. When we then turn on a smooth external gauge field inside the waveguide, the only light particle coupling to it is the right-handed fermion at the domain wall. For this scenario to work, we emphasize that the details of the conjectured phase diagram in fig. 2 are not important, but only that the PMS_1 phase exists. In the next section we shall investigate the scenario in more detail.

3 Mirror fermion representation of the model

3.1 Mode expansion

The colloquial discussion in the previous section can be made more explicit by rewriting the action as follows. Relabel the right and left handed fermion fields, $\Psi^s_{R,L} = P_{R,L}\Psi^s$ as

$$\begin{aligned} \psi^t_R &= \Psi^{s_0-1+t}_R, \;\; \psi^t_L = \Psi^{s_0-t}_L, \\ \chi^t_L &= \Psi^{s_0-1+t}_L, \;\; \chi^t_R = \Psi^{s_0-t}_R, \end{aligned} \tag{3.1}$$

and the same for $\overline{\Psi}_{R,L} = \overline{\Psi}P_{L,R}$ (note the reversal of L and R). The new label t runs from 1 to $L_t \equiv L_s/2$. In fig. 1 we have indicated this new labeling for the zeromode wave functions shown there. With our choice for s_0, s_0' and L_s we can define a domain wall mass for both fields ψ and χ, which is a step function in t satisfying,

$$\overline{m}^t = m^{s_0-1+t} = m^{s_0-t}. \tag{3.2}$$

With this relabeling the two domain wall zeromodes will reside in the Dirac fermion field ψ, whereas the waveguide boundary zeromodes will reside in χ. After substituting eq. (3.1) into eq. (2.8) with $U = 1$, the action turns into

$$\begin{aligned} S_{\psi\chi} &= \sum_{t=1}^{L_t} \left(\overline{\psi}^t \not{\partial} \psi^t + \overline{\chi}^t \not{\partial} \chi^t + \overline{\chi}^t (-w + \overline{m}^t) \psi^t + \overline{\psi}^t (-w + \overline{m}^t) \chi^t \right) \\ &- \sum_{t=1}^{L_t - 1} \left(\overline{\psi}^t \chi^{t+1} + \overline{\chi}^{t+1} \psi^t \right) + \sum_t \left(\overline{\chi}^t \psi^t + \overline{\psi}^t \chi^t \right) \\ &- y \overline{\chi}^1 (V P_L + V^\dagger P_R) \chi^1 - y \overline{\psi}^{L_t} (V^\dagger P_L + V P_R) \psi^{L_t}. \end{aligned} \tag{3.3}$$

In this form, the action resembles that of an L_t-flavor mirror fermion model in the fashion of ref. [28], with ψ the fermion and χ the mirror fermion field. In fact, for $L_s = 2$ the hopping terms in t are absent, $\overline{m}^t = 0$ and our model reduces to the mirror fermion model of ref. [28] with equal Yukawa couplings for the fermion and the mirror fermion, and a vanishing single-site mass term. For $L_s > 2$ our model has a more complicated mass matrix (i.e. nondiagonal couplings among the flavors s or t) and if our model is going to be more successful in decoupling the mirror fermion than the traditional mirror fermion approach, it must come from this mass term.

The mass matrix for the L_t flavors in our model is not diagonal but this can be remedied by more rewriting. First we expand the fermion fields in a plane wave basis, which diagonalizes the Dirac operator and Wilson term, $\psi_x^s = \sum_p e^{ixp} \psi_p^s$, $\overline{\psi}_x^s = \sum_p e^{-ixp} \overline{\psi}_p^s$. Here $\sum_p$ is a normalized sum over the momenta on the d dimensional lattice, $\sum_p 1 = 1$. Then we can write,

$$\begin{aligned} S_{\psi\chi} &= \sum_{t=1}^{L_t} \sum_p \left(i \overline{\psi}_p^t \not{s}_p \psi_p^t + i \overline{\chi}_p^t \not{s}_p \chi_p^t + \overline{\chi}_p^t (w_p + \overline{m}^t) \psi_p^t + \overline{\psi}_p^t (w_p + \overline{m}^t) \chi_p^t \right) \\ &- \sum_{t=1}^{L_t - 1} \left(\overline{\psi}_p^t \chi_p^{t+1} + \overline{\chi}_p^{t+1} \psi_p^t \right) + \sum_t \left(\overline{\psi}_p^t \chi_p^t + \overline{\chi}_p^t \psi_p^t \right) \\ &- y \sum_{pq} \left(\overline{\chi}_p^1 (V_{p-q} P_L + V_{q-p}^\dagger P_R) \chi_q^1 + \overline{\psi}_p^{L_t} (V_{q-p}^\dagger P_L + V_{p-q} P_R) \psi_q^{L_t} \right), \end{aligned} \tag{3.4}$$

with $\not{s}_p = \sum_\mu \gamma_\mu \sin(p_\mu)$, w_p the diagonal form of the Wilson term, $w_p = \sum_\mu (1 - \cos(p_\mu))$ and V_p the Fourier transform of V_x. For $y = 0$ the action has the schematic form

$$S_{\psi\chi} = (\overline{\psi}\ \overline{\chi}) \begin{pmatrix} i\not{s} & M^\dagger \\ M & i\not{s} \end{pmatrix} \begin{pmatrix} \psi \\ \chi \end{pmatrix}, \tag{3.5}$$

with M a (p dependent) matrix in flavor space, which can be read off from eq. (3.4). This action can be diagonalized by making unitary transformations on ψ and χ,

$$\begin{aligned} \omega^f &= F_{ft}^\dagger \psi^t, \quad \overline{\omega}^f = \overline{\psi}^t F_{tf}, \\ \xi^f &= G_{ft}^\dagger \chi^t, \quad \overline{\xi}^f = \overline{\chi}^t G_{tf}, \end{aligned} \tag{3.6}$$

such that $G^\dagger_{fs} M_{st} F_{tg} = \mu_f \delta_{fg}$. The matrices F and G are eigenfunctions of $M^\dagger M$ and $MM^\dagger$ respectively, labeled by the index f:

$$(M^\dagger M)_{st} F_{tf} = |\mu_f|^2 F_{sf}, \qquad (MM^\dagger)_{st} G_{tf} = |\mu_f|^2 G_{sf}. \tag{3.7}$$

For suitable choices of the phases of the eigenfunctions, the μ_f's are real. Substituting the mode expansion (3.6) into the action (3.4) with the momentum label restored, we arrive at

$$\begin{aligned} S_{\psi\chi} = &\sum_{f=1}^{L_t} \sum_p \left(\overline{\omega}^f_p i \not{s}_p \omega^f_p + \overline{\xi}^f_p i \not{s}_p \xi^f_p + \overline{\xi}^f_p \mu^f_p \omega^f_p + \overline{\omega}^f_p \mu^f_p \xi^f_p \right) \\ -y &\sum_{fg,pq} \left[\overline{\xi}^f_p G^{p\dagger}_{f1} (V_{p-q} P_L + V^\dagger_{q-p} P_R) G^q_{1g} \xi^g_q + \overline{\omega}^f_p F^{p\dagger}_{fL_t} (V^\dagger_{q-p} P_L + V_{p-q} P_R) F^q_{L_t g} \omega^g_q \right]. \end{aligned} \tag{3.8}$$

In this representation of the model, it is seen that all fermion modes ω^f and ξ^f interact with the scalar field, but that their effective Yukawa coupling is determined by the magnitude of their wave function at the waveguide boundaries $t = 1$ and $t = L_t$. For $y = 0$ the model is seen to describe free, degenerate fermions and mirror fermions with momentum dependent mass μ^f_p (for $\mu^f_p \neq 0$, the eigenstates are $\omega^f_p + \xi^f_p$ and $\omega^f_p - \xi^f_p$). Exactly one flavor, which we denote with $f = 0$, has $\mu^0_p = 0$ (up to terms exponentially suppressed in L_s) for $|\hat{p}| < p_c$, where p_c is the critical momentum defined in sect. 2.1. For $r = 1$ and m_0 close to 1, the critical momentum is $p_c \approx \sqrt{2}$. All other μ^f_p and also μ^0_p for p outside the critical momentum region, are $O(1)$ in lattice units. This is illustrated in fig. 3, where we show the lowest three masses as a function of the momentum (again we have chosen $d = 2$).

This shows that for $y = 0$ and momenta $|\hat{p}| \lesssim p_c$, the model contains a massless fermion, ω^0, as well as a massless mirror fermion, ξ^0. All other modes ($f \neq 0$) as well as the species doublers have a mass of the order of the cutoff. The species doublers of the zeromode $f = 0$ are massive because μ^0_p is $O(1)$ for momenta with $p_\mu = \pm\pi$. Furthermore, it is seen in fig. 3, that μ^0_p is almost exactly zero (it is exponentially small $\propto \exp(-m_0 L_s/4)$) until it quickly rises to nonzero values for $|\hat{p}| > p_c$.

As was discussed already in sect. 2.1, fig. 1 shows the t-dependence of the zeromodes F^{t0} and G^{t0} of the fermion (indicated by ψ in the figure) and mirror fermion (indicated by χ) for the smallest momenta $|p| = \pi/L \ll p_c$. It shows that the zeromode for the fermion is sharply peaked at $t = (L_t+1)/2$, i.e. at the domain wall and the zeromode for the mirror fermion is localized at the boundary, at $t = L_t$. The non-zeromodes, which are not shown in this figure, are not localized.

3.2 Reduced model

The action (3.8) is an exact representation of the action for the domain wall fermions. The reason for writing it in this form is that it reveals, more clearly than the original

action, which fermion modes are important for the low energy physics. To shed light on the model for $y \neq 0$, we shall exploit this separation of light and heavy modes in order to simplify the model by making a number of approximations, which we expect to hold for large L_s. First we shall neglect all non-zeromodes. This is a reasonable approximation, since these fermion modes have masses of the order of the cutoff, $\mu_p^f = O(1/a), f \neq 0$. If they would couple strongly to the zeromodes, they could still be important, but from the Yukawa interaction in (3.8) one can see that such a coupling involves the overlap of a zeromode and a non-zeromode at $t = 1$ or $t = L_t$. Since the non-zeromodes are not localized, the value of the wave functions $|G_{tf}|$ or $|F_{tf}|$ at any given t is of order $1/\sqrt{L_s}$ and the contribution of L_s internal heavy flavor fermions is expected to be of order $L_s|G_{1f}|^2/\mu_p^f = O(1/\mu_p^f)$.

The remaining zeromodes have a momentum dependent Yukawa coupling. For the fermion ω^0 this coupling is proportional to the squared absolute value of the wave function $F_{L_t 0}$ which is exponentially small. Furthermore, the mixing with the mirror fermion is either exponentially small for momenta $|\hat{p}| < p_c$, or the modes are very massive for large momenta $|\hat{p}| > p_c$, and we discard such heavy modes in our approximation. Therefore in this approximation the model describes a free massless fermion ω^0 with momentum cutoff at p_c, and a mirror fermion with Yukawa coupling to the scalar field. This Yukawa coupling contains a momentum dependent factor $G_{10}^{p\dagger} G_{10}^q$, cf. eq. (3.8). It turns out, however, that in the momentum range well below the cutoff p_c this factor is almost constant and close to one, and then quickly drops to a small value for $|\hat{p}| \gtrsim p_c$. This momentum dependence of $|G_{10}^p|$ is shown in fig. 4. This justifies the approximation that we also impose the momentum cutoff on the mirror fermion and neglect the wave function factor in the Yukawa coupling for $|\hat{p}| < p_c$.

All this leads to a simplified "reduced" model, described by the action

$$S^{red} = \sum_{|\hat{p}|<p_c} [i\overline{\omega}_p^0 \not{s}_p \omega_p^0 + i\overline{\xi}_p^0 \not{s}_p \xi_p^0] + y \sum_{|\hat{p}|,|\hat{q}|<p_c} \overline{\xi}_p^0 (V_{q-p}^\dagger P_R + V_{p-q} P_L) \xi_q^0. \qquad (3.9)$$

Notice that this model differs from the mirror fermion model of ref. [28] by the absence of a momentum dependent mixing term between fermions and mirror fermions and by the presence of the momentum cutoff $|\hat{p}| < p_c$.

In this approximation, the model shows all the features discussed in the previous section. In particular we see that the zeromode ω^0 which in the full model is localized at the domain wall, is nicely decoupled from the mirror fermion ξ^0 which is localized at the boundary. The domain wall zeromode has an exponentially small interaction with the scalar field, which we neglected in the action (3.9), but the mirror fermion couples to the scalar field with strength y. This mirror fermion will decouple if there exists a strong symmetric (PMS_1) phase for large y in which the mirror fermion and scalar field form a massive bound state. To summarize, the action (3.9) should describe the physics of the full model for $L_s \to \infty$, i.e. at the horizontal axis of the phasediagram in fig. 2.

The usual approach to show that such a phase exists is to write the action in terms of the fermion-scalar composite field,

$$\xi'_p = \sum_q (P_R \delta_{p,-q} + P_L V_{p-q}) \xi_q, \tag{3.10}$$

which is chosen such that the Yukawa term turns into a mass term for the fermion field ξ'. This fermion does not transform under the gauge group G, hence we shall call it neutral. If the momentum cutoff were absent, we could invert this transformation, $\xi_p = \sum_q (P_R \delta_{p,-q} + P_L V^\dagger_{q-p}) \xi'_q$, and a strong coupling approximation of the resulting action for ξ' would predict a mass of the order of the cutoff for this neutral fermion. However, due to the momentum cutoff such an argument cannot be used for our model and in fact the transformation (3.10) leads to a nonlocal action for ξ'.

The momentum cutoff, which prevents a straightforward analytic demonstration that a strong coupling phase exists, makes this model markedly different from models which are known to have a strong symmetric phase. It is somewhat similar, however, to a fermion-Higgs model with hypercubical Yukawa coupling [26, 29]. In these models the Yukawa interaction in momentum representation contains a momentum dependent factor, coming from the averaging of the scalar field over the hypercube, which suppresses the coupling strength for large values of the scalar field momentum. Such models are known not to have a strong symmetric phase.

To summarize this section, we have shown that the domain wall fermion model can be rewritten as a mirror fermion model, with $L_t = L_s/2$ flavors. In order to decouple the mirror partner of the domain wall zeromode, we must show the existence of a strong symmetric phase, where the mirror fermion forms a massive bound state with the scalar field. We have argued that the model for large L_s can be simplified to a reduced model with only a fermion and a mirror fermion. In this model we cannot show the existence of a strong phase using standard analytic techniques. The momentum dependence of the Yukawa interaction (which gives rise to the cutoff p_c) is more similar to that of a fermion-Higgs models with a hypercubical Yukawa interaction than to models with a local Yukawa interaction. Models with a hypercubical Yukawa interaction that have previously been investigated, are known not to have a strong symmetric phase.

Of course the similarity to hypercubically coupled fermion-Higgs models does not prove that a strong phase is absent in our model, and we shall search for it with numerical methods. The most direct way to show the existence of a strong coupling phase, is by measuring the mass of the boundary (mirror) fermion for strong Yukawa coupling. In the next section we shall study the fermion masses, both for the domain wall fermion and the boundary fermion, in the quenched approximation. We shall compare these results with the masses found from the reduced model.

4 Fermion spectrum: numerical results

In order to substantiate the discussion in the previous sections, we shall compute the fermion spectrum of the full domain wall model in the quenched approximation. We expect from experience gained with other fermion-Higgs models, that the presence of a strong coupling symmetric phase if it exists, can already be shown within the quenched model. In the quenched approximation there are no real phase transitions separating the PMW, PMS_1 and PMS_2 phases of fig. 2. One expects, however, that the FM phase separating these phases in the unquenched model, now turns into a cross-over region, which separates regions of the quenched phase diagram with different (weak and strong coupling) behavior. In the following we shall refer to these regions as weak and strong coupling phases, as in sect. (2.3).

For weak Yukawa coupling the mirror fermion mass in the quenched approximation is expected to behave as $m_F \approx yv$, where the scalar field expectation value v is zero in the symmetric phase and nonzero in the broken phase. A strong coupling symmetric phase would lead to $m_F = yc(\kappa)$, with $c(\kappa)$ a function of the scalar field hopping parameter κ. Typically $c(\kappa) > v(\kappa)$, it decreases with κ, and in particular it is nonzero and $O(1)$ in the symmetric phase. For instance, in the model of ref. [3], $c(\kappa) \approx 1/z(\kappa)$ with $z^2 \propto \mathrm{tr}\langle V_x V_{x+\mu}^\dagger \rangle$. For the domain wall fermion mass we expect $m_F \approx 0$ for all κ and $ye^{-m_0 L_s/4} \ll 1$.

For this numerical study we use the domain wall model in $2+1$ dimensions with gauge group $G{=}U(1)$, but we keep the gauge fields in the global symmetry limit $U = 1$. The scalar field action (2.11) then is that of an XY model, and in the quenched approximation, where the scalar field dynamics is determined solely by the action (2.11), there is a vortex phase and a spinwave phase. The Kosterlitz-Thouless phase transition is at $\kappa = \kappa_c \approx 0.5$ in our convention for the action. Of course spontaneous symmetry breaking does not really occur in this two dimensional model, but on a finite lattice the field expectation value v shows a behavior similar to that in a model with spontaneous symmetry breaking: it is nonzero and $O(1)$ for $\kappa > \kappa_c$ and then quickly drops to a small (nonzero) value for $\kappa < \kappa_c$. For increasing volumes v becomes closer to zero for $\kappa < \kappa_c$ but also in the spinwave phase it decreases slowly, such that in the limit of infinite volume $v = 0$ everywhere, as it should. We emphasize that in not too large volumes, in which there is a clear distinction between the value of v in the vortex and spinwave phases, we expect a similar relation between fermion mass and v as in a four dimensional model with spontaneous symmetry breaking. Hence we shall refer to the vortex phase as the symmetric phase and to the spinwave phase as the broken phase.

To find the fermion masses, we have measured the propagator in momentum space,

$$S^{st}(p) = L^{-2} \sum_{xy} e^{ip(x-y)} \langle \Psi_x^s \overline{\Psi}_y^t \rangle, \tag{4.1}$$

with L^2 the two dimensional lattice volume. Optimally, one should measure the full matrix $S^{st}(p)$ in flavor space, for a number of small momenta p and from that compute

the massive and massless eigenstates. However, the number of flavors typically is large (we use for instance $L_s = 26$), and it is impractical to compute the propagator matrix for all flavors s. Since we are only interested in the masses of the light states and since we know that these states are localized either at the domain wall or at the waveguide boundary, it is sufficient to compute only S^{ss} for selected s-values $s = 1, s_0-1, s_0, L_s/2+1, s_0'$ and $s_0'+1$. In fact, we know from the discussion in the previous section that the mirror fermion is localized near $s = s_0$ and we need only consider $s = s_0 - 1$ and s_0 if we are interested only in the mirror fermion mass.

The parity symmetry of eqs. (2.7) and (2.10) can be used, after averaging over the scalar field, to relate certain RR and LL components of the fermion propagator:

$$S^{st}_{RR}(p) = S^{L_t+2-s,L_t+2-t}_{LL}(Pp), \tag{4.2}$$

where Pp is the parity reflected two-momentum. We have used this relation to average over the appropriate RR and LL components, in order to increase statistics. For the RR or LL component of a free fermion propagator we expect

$$S(p)_{RR(LL)} = -iZ_F(\sin(p_1) - (+)i\sin(p_2))/(\sum_\mu \sin^2(p_\mu) + m_F^2), \tag{4.3}$$

where Z_F is a wave function renormalization constant and m_F is the mass. In fig. 5a we have plotted the inverse of the averaged RR and LL components, as a function of $\sum_\mu \sin^2(p_\mu)$. We used a lattice of size $L^2L_s = 12^226$ with Yukawa coupling $y = 0.5$, at $\kappa = 0.5$ near the phase transition and $m_0 = 1.1$. We used antiperiodic boundary conditions for the fermions in the t-direction. The data have been normalized such that the slope (determined from the first and second point) is one. The straight lines are χ^2 fits to the data and the good quality of these fits shows that the fermions are (nearly) free.

To see if the reduced model resembles the full model also in a quantitative way, we have computed the inverse mirror fermion propagator in this model. This result is shown in fig. 5b, again normalized to slope one. The normalized mirror fermion propagator is in good agreement with the one computed in the full model.

As anticipated the RR component of the domain wall fermion at $s = L_s/2 + 1$ (and the LL component at $s = 1$) has zero mass. The mirror fermion modes at $s = s_0-1$ (the RR component) and at s_0 (the LL component) have a small mass which is consistent with $m_F = yv$. All other components are seen to have a mass of order one in lattice units. In the same fashion we have computed the fermion masses at other values of κ and y. In all cases we found that the domain wall fermion remains massless.

Of course the most interesting results are those for the mirror fermion mass at small κ in the symmetric phase and at large values of y. Unfortunately, the data here are subject to large statistical fluctuations. Even after averaging over 3000 scalar field configurations at $\kappa = 0.1$ and $y = 10$ we found that the errorbars on the propagator are

comparable with the signal. The reason is that the propagator itself is very small, which prohibits a reliable analysis of the fermion propagator for such values of the couplings.

Instead of using $\kappa \approx 0$ such that $v \approx 0$, we can also look for strong coupling behavior at larger κ. In the broken phase the weak and strong regions are less pronounced, but the presence of a nearby PMS phase should still show up in a deviation from the relation $m_F \approx yv$. Since v decreases for $\kappa \searrow \kappa_c$, a characteristic feature of weak coupling behavior is a fermion mass which decreases as $\kappa \searrow \kappa_c$. As mentioned above, strong coupling behavior would show up through an opposite trend of the fermion mass as a function of κ, increasing towards the phase transition. In fig. 6 we show the κ dependence of the waveguide fermion mass at fixed $y = 2$. One recognizes the typical weak coupling behavior of the mass. From experience with other models we expect that $y = 2$ is already a strong coupling. For larger y it is difficult to measure the fermion mass reliably, because it is comparable to the cutoff in the range $\kappa \gtrsim 0.5$. In fig. 7 we have plotted the y dependence of the mass for fixed $\kappa = 0.5$. Strong coupling behavior should show up as a relative increase of the mass compared to the weak coupling trend. From fig. 7, however, we can at most infer a relative decrease of the mass for $y > 1$. For comparison, we have also plotted the line $yv(\kappa = 0.5)$ in this figure.

The crosses in figs. 6 and 7 are the masses obtained from the reduced model. One sees the same qualitative behavior as in the full model, but the masses are systematically higher (except when $m_F \gtrsim 2$, which is beyond the cutoff, where, in the full model, mixing with all the other heavy modes presumably becomes important). This difference may be due to the momentum dependence of the fermion wave function in the full model. For increasing momentum and masses closer to the cutoff, we expect the wave function to spread out and the overlap at the waveguide boundary to decrease. This implies that the residue Z_F of the fermion propagator (4.3) is not constant but decreases with increasing momentum. This also leads to an underestimate of the fermion mass in the full model. Keeping these systematic effects in mind, we consider the results of the reduced model in reasonably good agreement with the full model.

Even though at this stage we do not yet find a conclusive answer for κ deep in the symmetric phase and large Yukawa coupling, the results shown in figs. 5, 6 and 7, are consistent with the weak coupling mass relation $m_F = yv$. Also the awkward behavior of the model at small κ and large y is not what we expect from a model in the strong coupling phase. Only in the transition region between the two regimes we expect large statistical fluctuations, but after the bound state has formed, the model should describe weakly coupled massive Dirac fermions, whose mass should be easy to measure.

5 Search for a strong coupling symmetric phase

5.1 Eigenvalue spectra

The results for the mirror fermion mass described above are very suggestive but did not give a conclusive answer to the question whether a strong coupling phase exists in our model. Therefore we will attempt to approach this problem from a different angle in this section. The idea here will be that the presence of a strong coupling phase shows up in the distribution of the eigenvalues of the fermion matrix [30].

Of course, we would like to look at the eigenvalues of the domain wall fermion matrix directly. This $2L^2L_s \times 2L^2L_s$ (the factor 2 comes from the Dirac index) matrix M is obtained by writing the action (2.8), with $U = 1$, in the form $S = \overline{\psi}M\psi$. However, it is unpractical to study M directly, because this (nonhermitian) matrix is too large to handle numerically on reasonably sized lattices, and it is not clear what to expect for the distribution of the eigenvalues for M in the representation following from eq. (2.8). Only in the representation that diagonalizes the mass matrix in flavor space we should expect similarities with the eigenvalue spectra of free fermions (for small y) with momentum dependent masses.

This suggests that we use the reduced model, which is formulated in terms of these mass eigenstates, and which contains much less degrees of freedom. The reasonable agreement of the results for the fermion masses discussed in the previous section supports this strategy. In the reduced model we can compute the distribution of the eigenvalues of the fermion matrix at small, intermediate and large Yukawa coupling. Then we can compare these eigenvalue spectra with those obtained in models for which a strong coupling phase is known to exist or to be absent. As such reference models we use a model with naive fermions with local Yukawa coupling, which has a strong coupling phase, and the same model with hypercubical Yukawa coupling, which has no strong coupling phase. The actions for these models, which we shall refer to as the Y_{lc} and Y_{hc} models are,

$$S_{lc} = \sum_{xy} \overline{\psi}_x \partial\!\!\!/_{xy} \psi_y + y \sum_x \overline{\psi}_x (V_x P_R + V_x^* P_L) \psi_x, \tag{5.1}$$

$$S_{hc} = \sum_{xy} \overline{\psi}_x \partial\!\!\!/_{xy} \psi_y + y \sum_x \tfrac{1}{4} \sum_b \overline{\psi}_x (V_{x-b} P_R + V_{x-b}^* P_L) \psi_x. \tag{5.2}$$

The sum over b in the hypercubical Yukawa interaction runs over the four corners of the elementary plaquette, $b_\mu = 0, 1$. After Fourier transforming the Y_{hc} model, we find

$$S_{hc} = \sum_p \overline{\psi}_p i\not{s}_p \psi_p + y \sum_{pq} h_{p-q} \overline{\psi}_p (V_{p-q} P_R + V_{q-p}^* P_L) \psi_q \tag{5.3}$$

which contains a factor $h_{p-q} = \prod_\mu e^{i(p_\mu - q_\mu)/2} \cos((p_\mu - q_\mu)/2)$, which goes to zero for large momenta $|p_\mu - q_\mu| \to \pi$ of the V field.

The results of this comparison are presented in fig. 8. Fig. 8a contains the spectra of our reduced domain wall model at $\kappa = 0.1$ and $y = 0.2$, 1.0 and 4.0. We have plotted

the eigenvalues obtained from 5 quenched scalar field configurations, with lattice size $L = 12$. The figure shows that the scattering of the eigenvalues caused by the strongly fluctuating scalar field increases with increasing y, as expected. However, there is no sign of a qualitative change for larger y. Also for Yukawa couplings $y > 4$ we found that the spectra do not change qualitatively, they just scale proportionally to y.

This can be contrasted to the y dependence of the eigenvalue spectra in the Y_{lc} model shown in fig. 8b. Here we see an increase of the fluctuations for y growing from 0 to 1, then the eigenvalues λ start to rearrange themselves along the boundary of a crude circle, which cuts the real axis at approximately $\pm y$, such that the region around the origin becomes depleted of eigenvalues. This signals the existence of a strong coupling phase for $y \gtrsim 1$, cf. ref. [30].

The spectra of our reduced model do not show such a qualitative change for large y and are much similar to those shown in fig. 8c, which were obtained from the Y_{hc} model, and which does not have a strong coupling phase. Since we expect the reduced model to be qualitatively similar to the full model for large L_s, this result casts serious doubt on the existence of a strong coupling phase in our domain wall fermion model.

The properties of the eigenvalue distribution of the fermion matrix are also reflected in the behavior of the conjugate gradient (CG) inversion. For small Yukawa coupling and using anti-periodic boundary conditions to regulate the zeromode for the fermions, we expect a rapid convergence of the CG inversion on our relatively small lattice. Then for increasing y the inversion rate should deteriorate, i.e. the number of CG iterations to reach the solution to a given precision will increase. If there is a strong coupling phase, the number of iterations reaches a maximum at the cross-over to the strong phase and then decreases again, because in the strong coupling phase the composite fermions are again weakly coupled and massive. In ref. [27] it was found that the number of CG iterations provided an accurate indicator for the location of the cross-over and the existence of the strong coupling phase.

In fig. 9 we have plotted the number of CG iterations as a function of y at $\kappa = 0.1$ ($L = 12$, $L_s = 26$). One recognizes the expected rise of the number of iterations when y increases from 0 to ≈ 1.5. But, unlike what one expects for a model with a strong coupling phase, there is no decrease for large y. Also after $y = 2$ the number of iterations keeps rising, albeit at a slower rate and with larger fluctuations than at small y. For comparison we have also plotted the y dependence of the number of CG iterations obtained in the Y_{lc} and Y_{hc} model. In the Y_{lc} model, which has a strong coupling phase, the number of CG iterations clearly shows a peak at $y \approx 1$; in the Y_{hc} model, which has no strong coupling region, we see a behavior similar to that of our domain wall model.

We do not have an analytic method to establish the existence or nonexistence of a strong coupling phase in our model, but by comparing the Y_{lc} and Y_{hc} models, one might conjecture that a strong phase can only exist if the fermion and scalar modes are coupled strongly over the full momentum range, including the high momenta modes with p_μ near $\pm\pi$. This is the case in the Y_{lc} model, but both in the Y_{hc} model and in

our domain wall model the Yukawa coupling is suppressed for large momenta, though the details of the momentum dependence are different in the two models.

5.2 Dynamical fermions

We have also attempted an unquenched simulation of the model. A direct simulation of the model with the action (2.8), $S = \overline{\psi} M \psi$, is not feasible, because Det$M$ is not positive definite. Therefore we have simulated instead a model with an extra fermion field χ added, with action $S = \overline{\chi} M^\dagger \chi$, such that the fermion determinant is given by Det$(M^\dagger M)$. In this model we can use a hybrid Monte Carlo algorithm to include the fermions, because the fermion determinant is now manifestly positive definite.

To look for a strong coupling symmetric phase, one should use a small value of κ, such that the model is in the symmetric phase at $y = 0$. For $y > 0$ we expect that the system switches to the broken phase. This disappearance of the symmetric phase for arbitrarily small but nonzero y is a special feature of two dimensional Yukawa models, cf. e.g. [31] and references therein. Then for larger y we expect to find a symmetric phase if such a phase exists. Unfortunately, the system turns out to be extremely hard to simulate numerically for small κ. For $\kappa = 0$ and small y we could still measure nonzero field expectation values, but for increasing y we had to decrease the trajectory length progressively more, to unacceptably small values (e.g. at $y = 1$ we had to use a step size $dt = 0.01$ with 10 steps per trajectory to maintain an acceptance rate larger than 75%, and at $y = 10$ we had to use $dt = 0.001$). This results in huge autocorrelation and equilibrium times, which make a realistic simulation unfeasible for values of y in the interesting region. Presumably this is due to large fluctuations in the eigenvalues of $M^\dagger M$, as is suggested by the spectra of the reduced model shown in fig. 8. In fig. 9 we have also plotted the number of CG iterations required for inversions in the unquenched model at $\kappa = 0$ (full triangles). This shows the same steady increase with y as found in the quenched model. Also a tentative run at $y = 10$, showed none of the improvement we would expect after moving into a strong coupling phase.

6 Other ways to couple the gauge fields

The model we have studied in this paper resulted from an attempt to couple gauge fields to the chiral mode on only one of the domain walls, while preserving gauge invariance. This gave rise to an extra scalar field and additional mirror fermion modes at the waveguide boundary. These mirror fermion modes do not seem to decouple, in other words, there does not seem to exist a region in the phase diagram where the mirror fermions have masses of the order of the cutoff, while the zeromodes at the domain walls remain light. However, one might wonder whether the gauge field cannot be coupled to the fermions in a different way, which avoids these complications. Unfortunately, it

appears to be difficult to find a different approach without obvious flaws. Let us briefly discuss the original proposal [12], and its relation to the model studied in this paper.

In the original proposal gauge fields were put on all links of the $d+1$ dimensional lattice, i.e. the gauge field was taken to be a full, $d+1$-dimensional gauge field. The action for these gauge fields was chosen as

$$S(U) = \sum_{x,s} \left(\beta \sum_{\mu,\nu=1}^{d} \mathrm{Re\ tr}\,(U^s_{\mu x} U^s_{\nu x+\hat{\mu}} U^{s\dagger}_{\mu x+\hat{\nu}} U^{s\dagger}_{\nu x}) + \beta_{d+1} \sum_{\mu} \mathrm{Re\ tr}\,(U^s_{\mu x} V^s_{x+\hat{\mu}} U^{s+1\dagger}_{\mu x} V^{s\dagger}_x) \right). \tag{6.1}$$

The gauge field in the $d+1$ direction is denoted by V. By choosing the coupling β_{d+1} for the extra field V sufficiently different from the plaquette coupling β for the gauge fields U^s, it was hoped that at the domain wall the gauge field dynamics would still be d-dimensional at scales much below the cutoff.

Eq. (6.1) can be viewed as the action for a number of d-dimensional gauge fields U^s (labeled by s), coupled to equally many unitary scalar fields V^s. For $U^s = 1$ we have just L_s independent nonlinear sigma models in d dimensions, each with a critical point at $\beta_{d+1} = \beta_c$. For each s, the global symmetry group is $G \times G$, with V^s transforming as

$$V^s \to g^s V^s (g^{s+1})^\dagger, \tag{6.2}$$

with the g^s in G. The full symmetry group $\mathcal{G} = G^{L_s}$ is gauged by the d-dimensional gauge fields U^s. The hopping terms in the s-direction in the fermionic part of the action look like the Yukawa terms in our model, eq. (2.8) (with $y = 1$):

$$S_{\Psi V} = -\sum_s (\overline{\Psi}^s V^s P_L \Psi^{s+1} + \overline{\Psi}^{s+1} V^{s\dagger} P_R \Psi^s). \tag{6.3}$$

For $U^s = 1$ and $\beta_{d+1} < \beta_c$, the symmetry $\mathcal{G}$ is unbroken, and $\langle V^s_x \rangle = 0$ for all s. It is then easy to see that in a mean field approximation, where V^s_x is replaced by $v = 0$, the fermion action is that of 2 massless Wilson fermions and $L_s - 2$ Wilson fermions with mass $\approx m_0$, which are decoupled from each other, and vectorlike in d dimensions. This has been investigated in more detail in ref. [22].

If we now take $\beta_{d+1} > \beta_c$, the group $\mathcal{G}$ breaks down to its diagonal subgroup, $G^{L_s} \to G$, and only one gauge field remains massless. The other gauge fields would get a mass $\propto v = \langle V \rangle$, and could be made very massive by choosing v at the cutoff. The fermion hopping terms in the s direction would survive (in mean field), and we would find the usual zeromodes at both domain walls. However, the massless gauge field is independent of s and couples equally to the modes at the domain and anti-domain walls, again rendering the model vectorlike.

In a sense then, the model which we studied in this paper, is an improvement on this situation. Formally, our model corresponds to choosing $\beta_{d+1} = \infty$ for all but two s-slices (where we set $\beta_{d+1} = \kappa$), forcing the $d+1$-dimensional gauge field to be d-dimensional.

There is no interaction with the antidomain wall if we choose the plaquette coupling $\beta = \infty$ outside the waveguide.

In our model we have chosen an s-dependence of β_{d+1} and β, (and of the fermion hopping parameter in the s-direction by the introduction of a Yukawa coupling $y \neq 1$ at the waveguide boundary), which we think had the best chance of producing a chiral model. Of course, a more general s-dependence is possible, but we do not believe that this will improve the situation as described in this paper.

7 Summary and conclusion

In this paper we have considered a gauge theory with domain wall fermions in a finite volume with a right-handed zeromode living at the domain wall and a left-handed zeromode at the anti-domain wall. The right-handed mode at the domain wall is coupled to a four dimensional gauge field which is confined to a waveguide around this domain wall. The left-handed mode at the anti-domain wall remains uncoupled [24]. The fermion hopping terms across the waveguide boundaries break gauge invariance, which is restored by promoting these hopping terms to Yukawa couplings in a way similar to the way fermion mass terms are made gauge invariant in the Standard Model. This leads to the introduction of a scalar field which lives only at the boundaries of the waveguide. There are two parameters in this model associated with this scalar field, a Yukawa coupling y and a hopping parameter κ (or equivalently a mass) for the scalar field. In our numerical work we have studied the scalar-fermion dynamics in the model with U(1) gauge symmetry in $2+1$ dimensions. The gauge fields, which can be treated perturbatively, are switched off and we mainly used the quenched approximation.

For vanishing Yukawa coupling the regions inside and outside the waveguide decouple from each other and from the scalar field. Therefore one would expect that new chiral zeromodes show up at the waveguide boundaries. This is indeed what happens: there is a left-handed mirror mode just on the inside of one of the waveguide boundaries, and a right-handed mirror mode on the outside (cf. fig. 1). The inside mirror fermion couples to the gauge field in the waveguide, resulting in a vectorlike theory. To show explicitly that our domain wall fermion model can be interpreted as a mirror fermion model, one can view the extra dimension as a flavor space. The hopping and single site terms in the extra dimension then generate a mass matrix, which is not diagonal in flavor space. By diagonalizing this mass matrix at $y = 0$, one recovers the massless domain wall modes as well as the massless mirror partners at the waveguide boundary. All other modes have masses of the order of the cutoff. For $y \neq 0$ all modes have Yukawa interactions with the scalar field, proportional to y and to the magnitude of the wave function of the particular mode at the waveguide boundary. Since the wave function of the domain wall mode is exponentially small at the waveguide boundary, its Yukawa interaction is very weak, even at large values of y; the mirror mode, however, interacts strongly with

the scalar field.

The crucial question is then whether the mirror fermion can be decoupled. A favorable possibility would be that for large Yukawa coupling, the mirror fermion at the waveguide boundary forms a bound state with the scalar field, with a Dirac mass of the order of the cutoff, while the gauge symmetry remains unbroken. Such a strong coupling behavior is known to exist in many fermion-scalar models. In particular a strong symmetric or paramagnetic (PMS) phase has been established in these models. The key point in our model is that only the mirror fermion should become heavy, while the modes at the domain walls should remain massless. This would be conceivable, because the mirror mode couples much more strongly to the scalar field than the domain wall mode.

One might ask whether such a scenario is excluded by the simple consideration that the massless mirror mode is required to cancel the anomaly generated by the domain wall mode. We think that this is not the case. If one turns on a smooth external gauge field, a Goldstone-Wilczek current will carry charge away from the domain wall. However, since no gauge field is present outside the waveguide, this current vanishes in that region, and the charge will have to be deposited somehow at the waveguide wall. Of course, if massless mirror fermions are present, they will do the job, much as the antidomain wall zeromodes did in the case without a waveguide, but rather with an external gauge field present throughout space-time [12, 15, 18]. However, an alternative possibility is that a Wess-Zumino current carries the charge at the waveguide without any massless fermion modes being present. In the $V = 1$ gauge (where V is the scalar field), a charge density of the form $j_0 \propto \epsilon_{0ij}\partial_i A_j$ can be nonzero due to the discontinuity of the gauge potential A at the waveguide boundary.

In our numerical work we have used several approaches to search for the existence of a PMS phase, but never found an indication that it exists. Our best evidence that it is absent, comes from computations of the mirror fermion mass at values of κ near the phase transition to the symmetric phase, where the dependence of the mirror fermion mass on κ and y is consistent with the weak coupling mass relation $m_F = yv$ even for large values of y (v is the scalar vacuum expectation value). No sign of the behavior typical of a strong Yukawa coupling region was found (cf. figs. 6 and 7). For all values of the Yukawa coupling that we have considered, the domain wall zeromodes remain massless and unaffected by the Yukawa interactions. It would of course be nice to directly measure fermion masses deep in the symmetric phase, for small κ and large y. However, in this parameter region the signal for the propagator disappears in the noise and we have not been able to obtain data with small enough errors to draw any definite conclusion about the mirror fermion mass.

Since direct computations of the mirror fermion mass run into numerical difficulties, we have also studied a "reduced" model, which contains only the mirror fermion interacting with the scalar field. It is obtained from the full model for large L_s (the extent in the extra dimension) by discarding all fermion modes with masses of the order of

the cutoff. Since the Yukawa coupling of the domain wall zeromode is exponentially suppressed in L_s, this mode can also be discarded. The momentum dependence of the mirror fermion wave function is such that the effective Yukawa coupling for this mode is suppressed for momenta larger than the critical momentum p_c and hence we also discard these large momentum modes. We computed the eigenvalue spectrum of the fermion matrix for this reduced model as a function of y, and compared this with typical eigenvalue spectra for simple Yukawa models. The eigenvalue spectra of such models are very different for large y, depending on whether a PMS phase does or does not exist [30]. The eigenvalue spectrum of the reduced model shows no sign of a PMS phase (cf. fig. 8).

Of course, one would like to study the eigenvalue spectrum of the full model directly. This was not possible due to the prohibitive amount of computer resources that would be needed. We believe however, that the "reduced" model captures the essential features of the full model, one of which is the existence of an effective momentum cutoff at p_c. This belief is supported by a reasonable agreement between light fermion masses computed in the full and reduced models.

It appears that the existence of an effective momentum cutoff p_c in the theory, is the underlying reason for the failure to find a PMS phase. In the domain wall approach the fermion doublers are decoupled by making them heavy which implies that these modes are not bound to the domain wall or waveguide boundary, as is the case with the light modes. This implies that for large momenta near the doubler momenta $p_\mu = \pi$, the wave function of the boundary mode will be spread out in the extra dimension and it will be small at the location of the scalar field. Therefore the effective Yukawa coupling for these large momenta modes is necessarily small. However, this suppression of the Yukawa coupling for large momenta then prevents the formation of fermion-scalar field bound states necessary to have a strong coupling phase. As a result, the mirror fermion at the waveguide boundary stays light, and renders the theory vectorlike in the scaling region. If this picture is right, it points at a fundamental problem for domain wall fermions with a waveguide, not just for the two dimensional quenched U(1) model investigated here.

The results discussed above were obtained in the quenched approximation. The unquenched model, assuming the decoupling of the boundary fermion would have been successful, would describe a single right handed fermion interacting with a U(1) gauge field. This model is anomalous and one might fear that our unfavorable results are a reflection thereof. This, however, is not likely, because we can also think of our model as the quenched approximation of a vectorlike model, obtained by adding an extra mirror fermion: writing the original action (2.8) as $S = \overline{\psi} M \psi$, we can add an extra fermion field χ with action $S = \overline{\chi} M^\dagger \chi$. For the additional χ fermion, the handedness of the zeromodes at the domain wall and waveguide boundary is reversed and the model is now anomaly free. In the quenched approximation, however, the extra fermion is irrelevant and this model reduces to the one studied here.

We have performed some unquenched simulations in the model with the extra fermion included, using a hybrid Monte Carlo algorithm. The results are inconclusive due to the very large autocorrelation and equilibration times, but do not contradict the conclusions described above.

All our numerical computations have been carried out within a restricted range of Yukawa couplings, as typically the signal to noise ratio deteriorated prohibitively for large values of y in the symmetric phase. Therefore, it is not logically excluded that some PMS like behavior might be found at values of y beyond $y \approx 10$ or so. In particular, we have not tried to investigate the existence of a PMS_2 phase as described in section 2.3. This phase would not be interesting, however, for the construction of a chiral gauge theory, since also the domain wall zeromodes would be strongly coupled to the scalar field and neutral with respect to the gauge charge.

To summarize, we believe that all the evidence presented in this paper — the close resemblance to a mirror fermion model with hypercubical Yukawa interaction, the κ and y dependence of the mirror fermion mass where we could measure it, the distribution of the eigenvalues in the reduced model for large y and the behavior of the conjugate gradient algorithm — indicates that a PMS phase does not exist in our model and that the mirror fermions, which exist as a consequence of the introduction of a waveguide, cannot be made heavy. Therefore, a vectorlike gauge theory will result when gauge interactions are turned on. In view of the discussion in section 6, we expect that this negative result is quite general for domain wall fermion models in which the volume in the extra dimension is kept finite at any stage in the definition of the model.

Acknowledgements:

We would like to thank D. Kaplan for many stimulating discussions and valuable suggestions. We would also like to thank G. Bodwin, A. De, A. Gonzalez-Arroyo, J. Kuti and R. Narayanan for discussions. M.G. would like to thank the Physics Department of UC San Diego, and K.J. that of Washington University for hospitality. This work is partially supported by the DOE under grants DE-FG03-91ER40546 and DOE-2FG02-91ER40628, and by the TNLRC under grant RGFY93-206. The numerical computations were performed on the Cray Y-MP8/864 at the San Diego Supercomputer Center.

References

[1] L.H. Karsten and J. Smit, Nucl. Phys. B183 (1981) 103.

[2] H. B. Nielsen and M. Ninomiya, Nucl. Phys. B185 (1981) 20; erratum: Nucl. Phys. B195 (1982) 541; Nucl. Phys. B193 (1981) 173; Phys. Lett. 105B (1981) 219; L. H. Karsten, Phys. Lett. 104B (1981) 315; D. Friedan, Comm. Math. Phys. 85 (1982) 481.

[3] J. Smit, Acta Physica Polonica B17 (1986) 531 (Zakopane 1985);
L.H. Karsten, in Field Theoretical Methods in Particle Physics, ed. W. Rühl, Plenum (1980) (Kaiserslautern 1979);
J. Smit, Nucl. Phys. B175 (1980) 307;
P.D.V. Swift, Phys. Lett. B145 (1984) 256.

[4] E. Eichten and J. Preskill, Nucl. Phys. B268 (1986) 179.

[5] C. Pryor, Phys. Rev. D43 (1991) 2669.

[6] S.V. Zenkin, Univ. of Zaragoza preprint DFTUZ/92/7 (1992);
Nucl. Phys. B (Proc. Suppl.) 30 (1993) 613.

[7] J. Smit, Nucl. Phys. B (Proc. Suppl.) 4 (1988) 451. J. Smit, Nucl. Phys. B (Proc. Suppl.) 26 (1992) 480. J. Smit, Nucl. Phys. B (Proc. Suppl.) 29B,C (1992) 83.

[8] J.L. Alonso, P. Boucaud, J.L. Cortes and E. Rivas, Mod. Phys. Lett. A5 (1990) 275; Nucl. Phys. (Proc. Suppl.) 17 (1990) 461.

[9] A. Borrelli, L. Maiani, G.C. Rossi, R. Sisto and M. Testa, Phys. Lett. B221 (1989) 360; Nucl. Phys. B333 (1990) 355.

[10] G.T. Bodwin and E.V. Kovacs, Nucl. Phys. B (Proc.Supp.) 20 (1991) 546; Nucl. Phys. B (Proc.Supp.) 30 (1993) 617.

[11] M. Göckeler and G. Schierholz, Nucl. Phys. B (Proc. Suppl.) 29B,C (1992) 114.

[12] D.B. Kaplan, Phys. Lett B288 (1992) 342.

[13] S.A. Frolov and A.A. Slavnov, preprint MPI-Ph 93-12.

[14] D.N. Petcher, Nucl. Phys. B (Proc. Suppl.) 30 (1993) 50.

[15] K. Jansen, Phys. Lett. B288 (1992) 348.

[16] Z. Yang, Phys. Lett. B 296 (1992) 151.

[17] K. Jansen and M. Schmaltz, Phys. Lett. B 296 (1992) 374.

[18] M.F.L. Golterman, K. Jansen and D.B. Kaplan, Phys. Lett. B301 (1993) 219.

[19] Y. Shamir, Phys. Lett. B 305 (1993) 357; Weizmann Inst. preprint, WIS-93-20-PH, hep-lat 9303005.

[20] R. Narayanan and H. Neuberger, Phys. Lett. B302 (1993) 62; Rutgers preprint RU-93-25 and RU-93-34.

[21] J. Distler and S-J. Rey, Princeton preprint PUPT-1386.

[22] C.P. Korthals-Altes, S. Nicolis and J. Prades, Marseille preprint CPT-93-P-2920.

[23] C.G. Callan Jr. and J.A. Harvey, Nucl. Phys. B250 (1985) 427.

[24] D.B. Kaplan, Nucl. Phys. B (Proc. Suppl.) 30 (1993) 597

[25] A. Hasenfratz and T. Neuhaus, Phys. Lett. B220 (1989) 435.

[26] J. Shigemitsu, Nucl. Phys. B (Proc. Suppl.) 20 (1990) 515.

[27] W. Bock, A.K. De, K. Jansen, J. Jersák, T. Neuhaus and J. Smit, Nucl. Phys. B344 (1990) 207.

[28] I. Montvay, Phys. Lett. B199 (1987) 89; Nucl. Phys. B (Proc. Suppl.) 29B,C (1992) 159.

[29] I-H. Lee, J. Shigemitsu and R.E. Shrock, Nucl. Phys. B330 (1990) 225.

[30] I. Barbour, W. Bock, C. Davies, A.K. De, D. Hently, J. Smit and T. Trappenberg, Nucl. Phys. B368 (1992) 390.

[31] A.K. De, E. Focht, W. Franzki, J. Jersák and M.A. Stephanov, Phys. Lett. B308 (1993) 327.

Figure captions

Fig. 1: Wave functions of the four lightest modes with momentum $|p| = \pi/L$, on a $2+1$ dimensional lattice with $L = 18$, $L_s = 50$ and $m_0 = 1.1$. The solid (dotted) lines represent right (left) handed components. The ψ and χ are the fermion and mirror fermion located at the domain wall (vertical bar) and waveguide boundary (dashed band) respectively. We indicate both the s and t labeling defined in eq. (3.1). Figure a is for $y = 0$, figure b for y=0.5.

Fig. 2: Sketch of a phase diagram which would make the the domain wall fermion model successful. The y and $ye^{-m_0 L_s/4}$ indicate the effective Yukawa couplings for the domain wall and waveguide fermion respectively and $\kappa = 0$. The various phases are explained in sect. 2.3.

Fig. 3: Momentum dependence of the three lowest mass eigenvalues μ^f at $y = 0$, obtained on a $2+1$ dimensional lattice with $L = 16$, $L_s = 50$ and $m_0 = 1.1$. The domain wall fermion and waveguide fermion have degenerate masses.

Fig. 4: Momentum dependence of the three wave functions $|G_{f1}|$ corresponding to the eigenvalues μ^f shown in fig. 3, evaluated at the waveguide, $t = 1$, on a $2+1$ dimensional lattice with $L = 16$ and $L_s = 50$ and $m_0 = 1.1$. The symbols correspond to those of fig. 3.

Fig. 5: Inverse propagator $S^{-1}(p)$ measured at $s = 1$, $s_0 - 1$, s_0, $L_s/2+1$, s_0' and $s_0'+1$, for $y = 0.5$ and $\kappa = 0.5$ on a $12^2 26$ lattice with $m_0 = 1.1$. We show averaged components as explained in the text, errorbars are smaller that the symbols. For free naive fermions the fits with Ansatz $S^{-1}(p) = (m_F^2 + \sum_\mu \sin^2 p_\mu)/Z_F$ (solid lines) would be exact. Figure a is for the full model which has the domain wall zeromode (squares), the light waveguide mode (triangles) and many heavy modes (circles); figure b is for the reduced model, which only contains the waveguide mode.

Fig. 6: The κ dependence of the waveguide fermion mass at strong coupling $y = 2$, on a $12^2 26$ lattice with $m_0 = 1.1$. The boxes (crosses) are for the full (reduced) model.

Fig. 7: The y dependence of the waveguide fermion mass near the phase transition at $\kappa = 0.5$, on a $12^2 26$ lattice with $m_0 = 1.1$. The boxes (crosses) are for the full (reduced) model.

Fig. 8: Eigenvalue spectra for the reduced domain wall fermion model (figures a), the reference Yukawa model with local (figures b) and hypercubical (figures c) coupling. The left, middle and right figures are for $y = 0.2$, 1.0 and 4.0 respectively. The lattice size is $L^2 = 12^2$ and $\kappa = 0.1$.

Fig. 9: Number of conjugate gradient iterations to reduce the residual to $< 10^{-6}$. The full symbols are for the quenched (circles) and unquenched (triangles) domain wall fermion model on a $12^2 26$ lattice. The open symbols are for the Yukawa models defined in eq. (5.2) with local (triangles) and hypercubical (boxes) Yukawa interaction, on a 12^2 lattice with $\kappa = 0.1$.

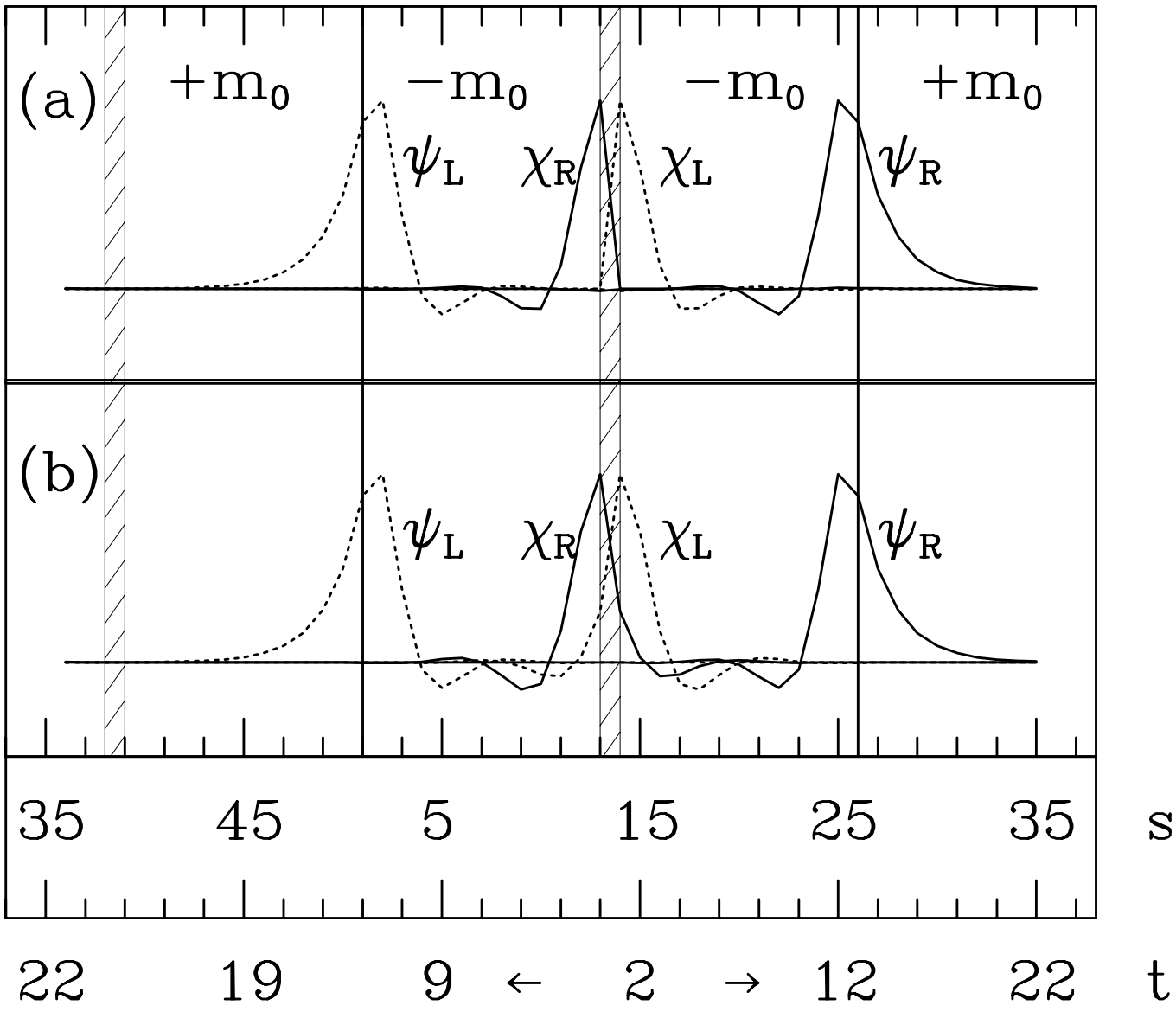

Fig.1

This figure "fig1-1.png" is available in "png" format from:

http://arXiv.org/ps/hep-lat/9309015v1

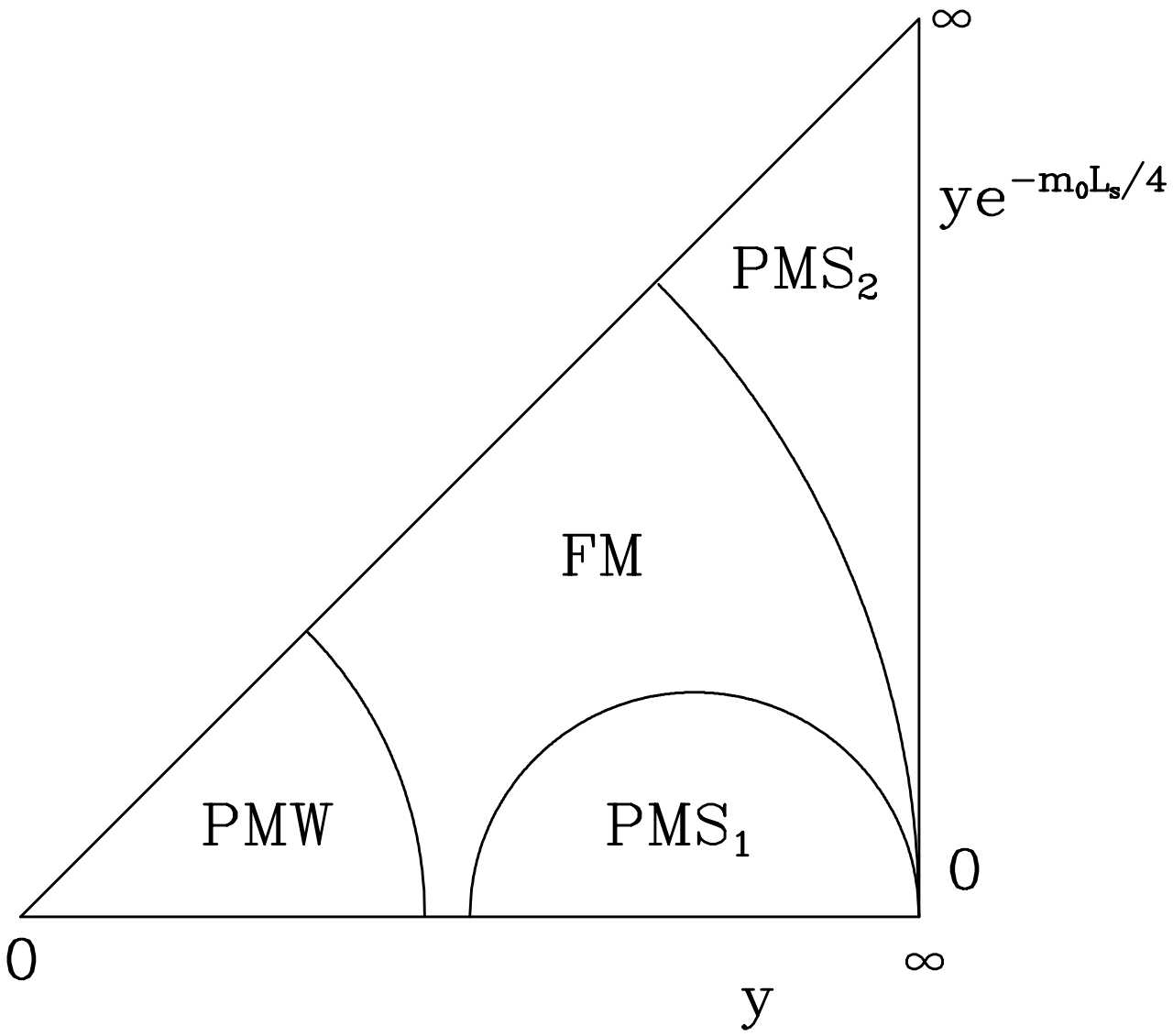

Fig.2

This figure "fig1-2.png" is available in "png" format from:

http://arXiv.org/ps/hep-lat/9309015v1

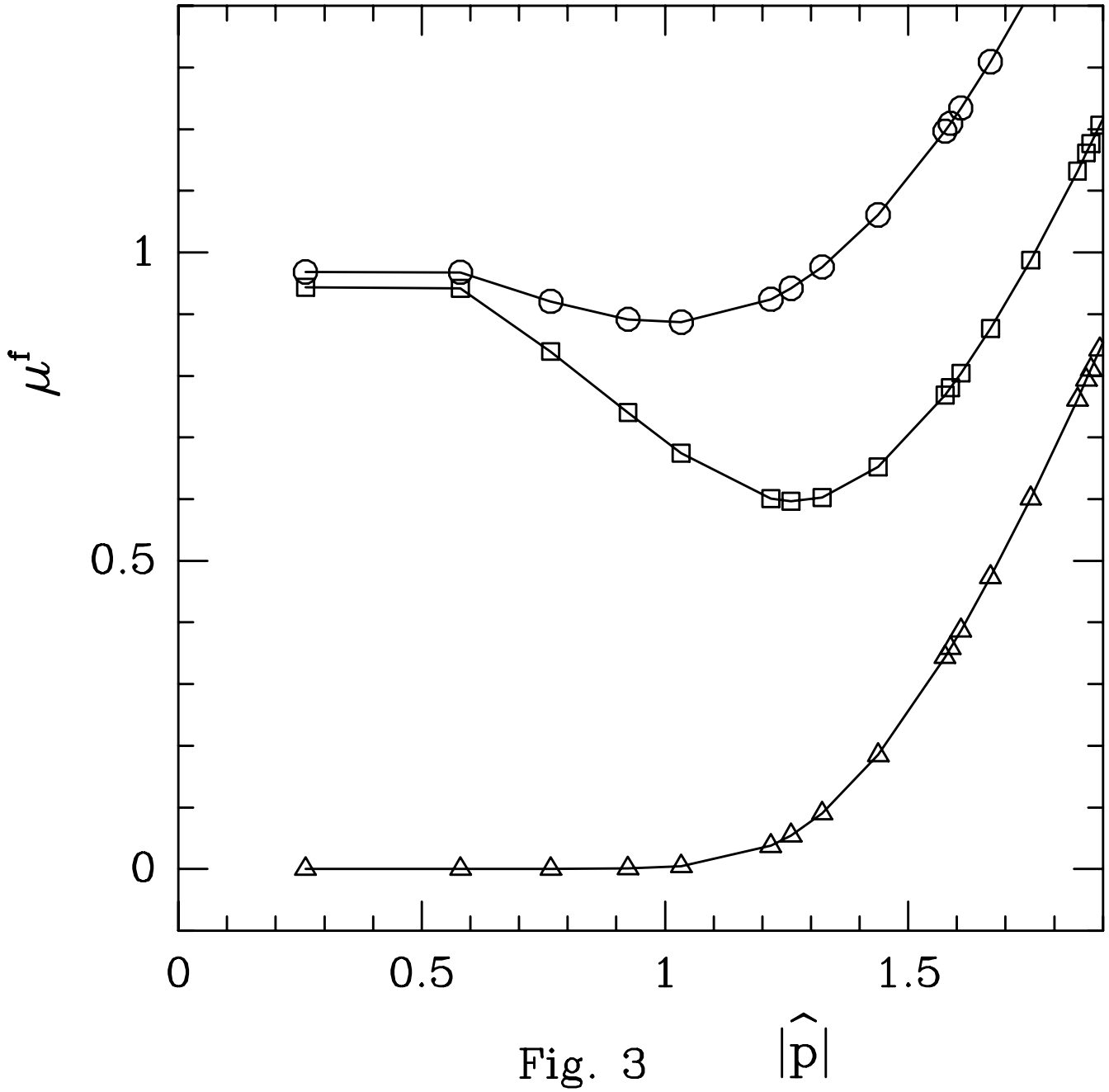

Fig. 3

This figure "fig1-3.png" is available in "png" format from:

http://arXiv.org/ps/hep-lat/9309015v1

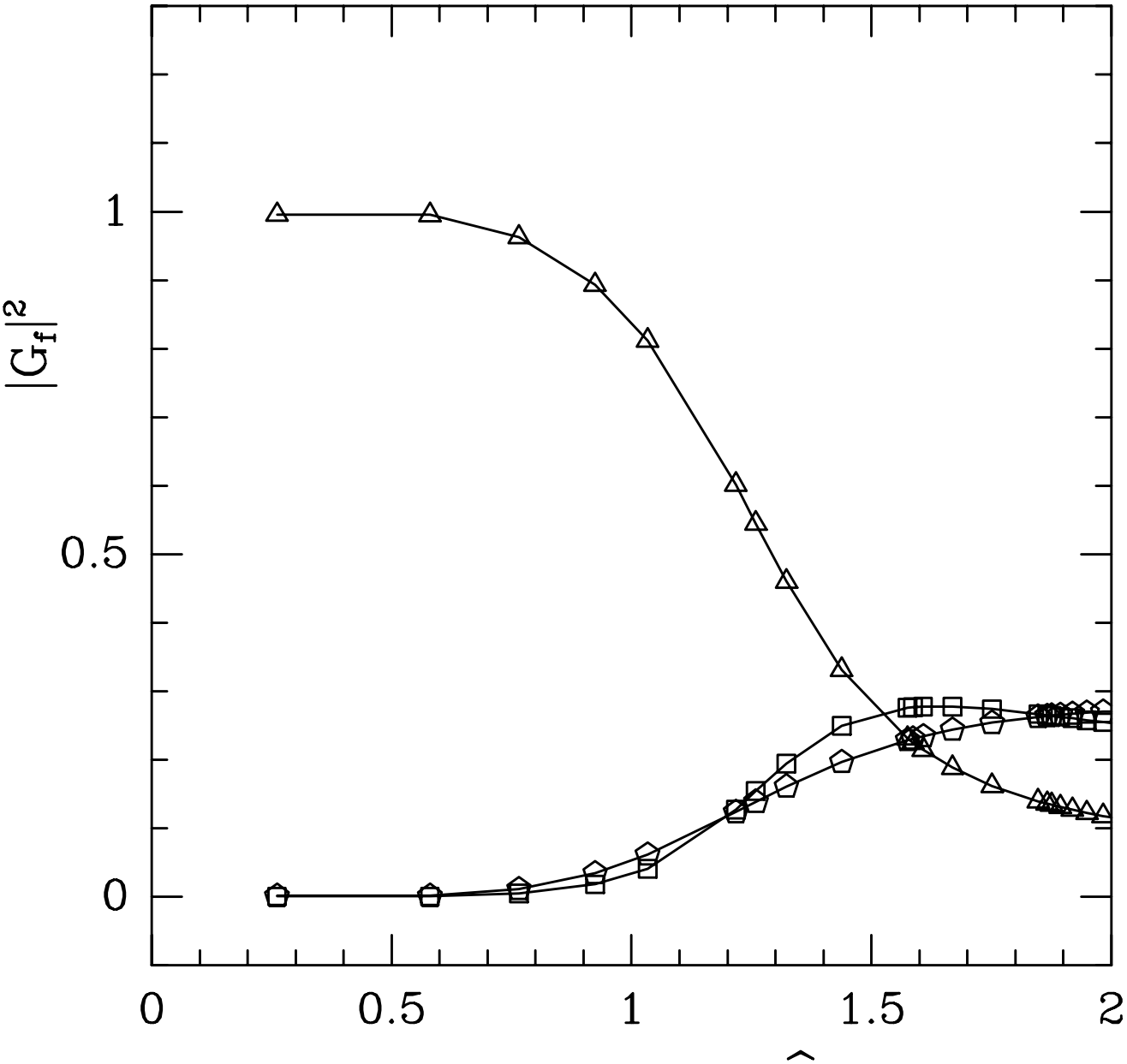

Fig. 4

This figure "fig1-4.png" is available in "png" format from:

http://arXiv.org/ps/hep-lat/9309015v1

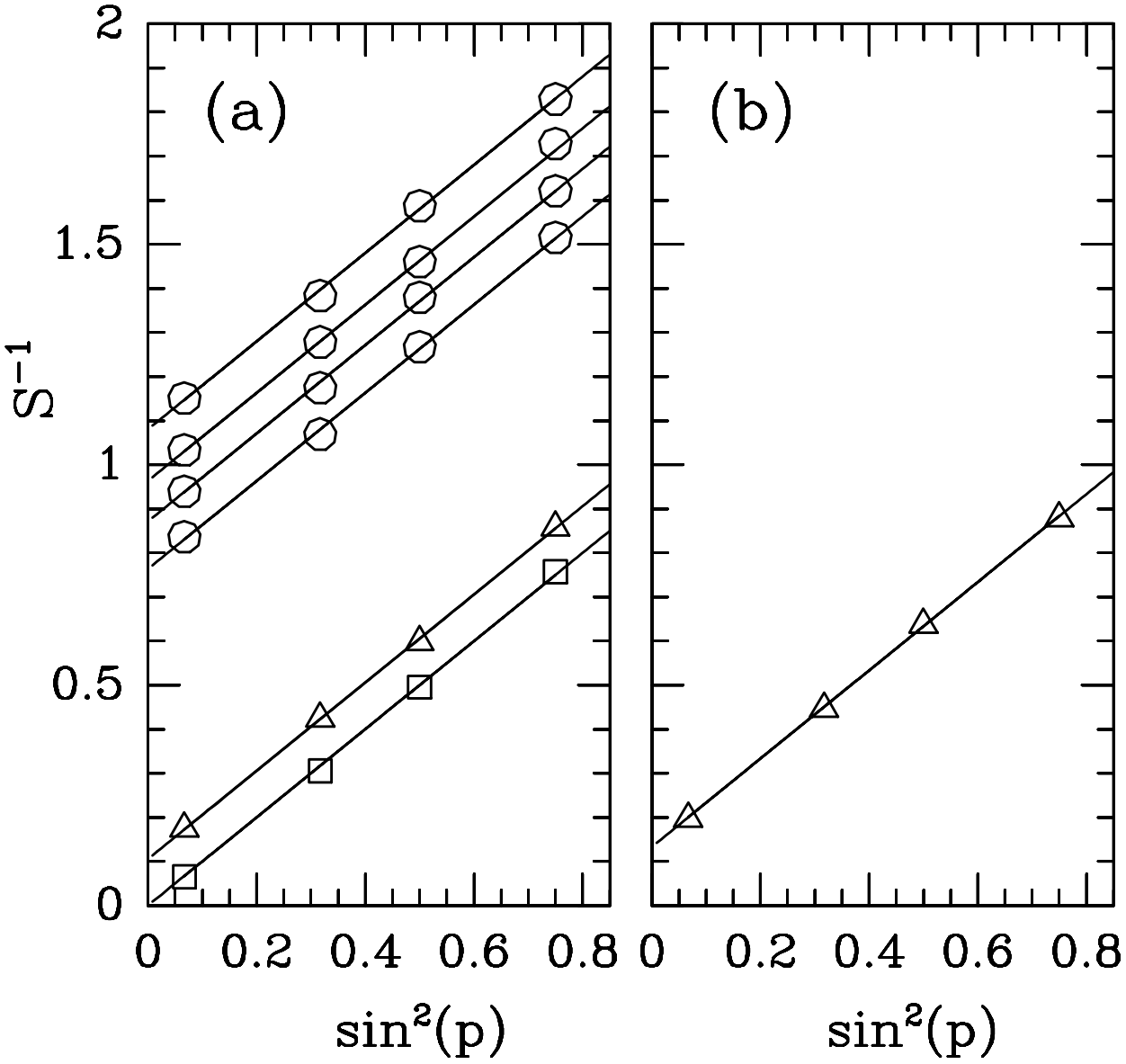

Fig. 5

This figure "fig1-5.png" is available in "png" format from:

http://arXiv.org/ps/hep-lat/9309015v1

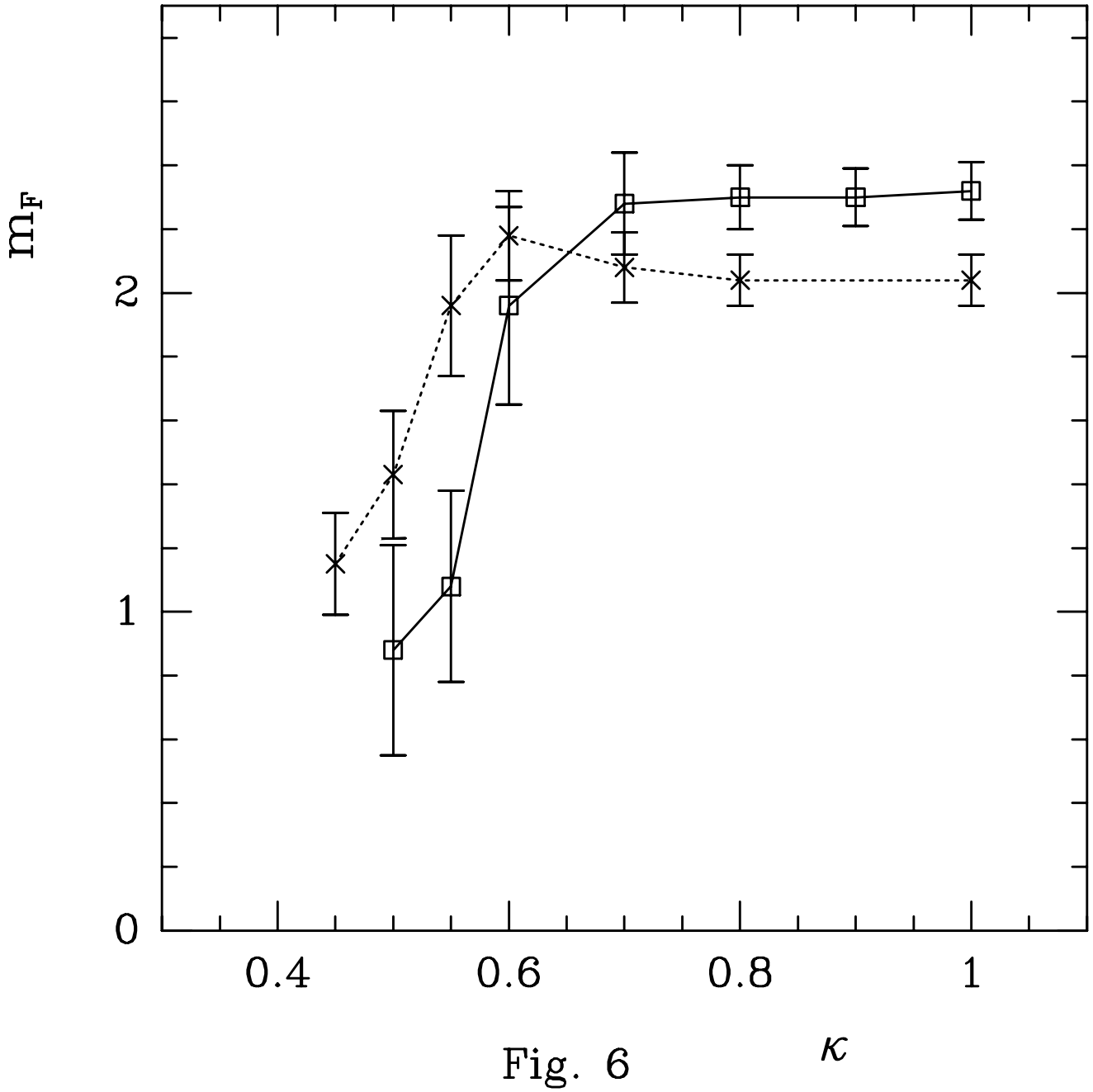

Fig. 6

This figure "fig1-6.png" is available in "png" format from:

http://arXiv.org/ps/hep-lat/9309015v1

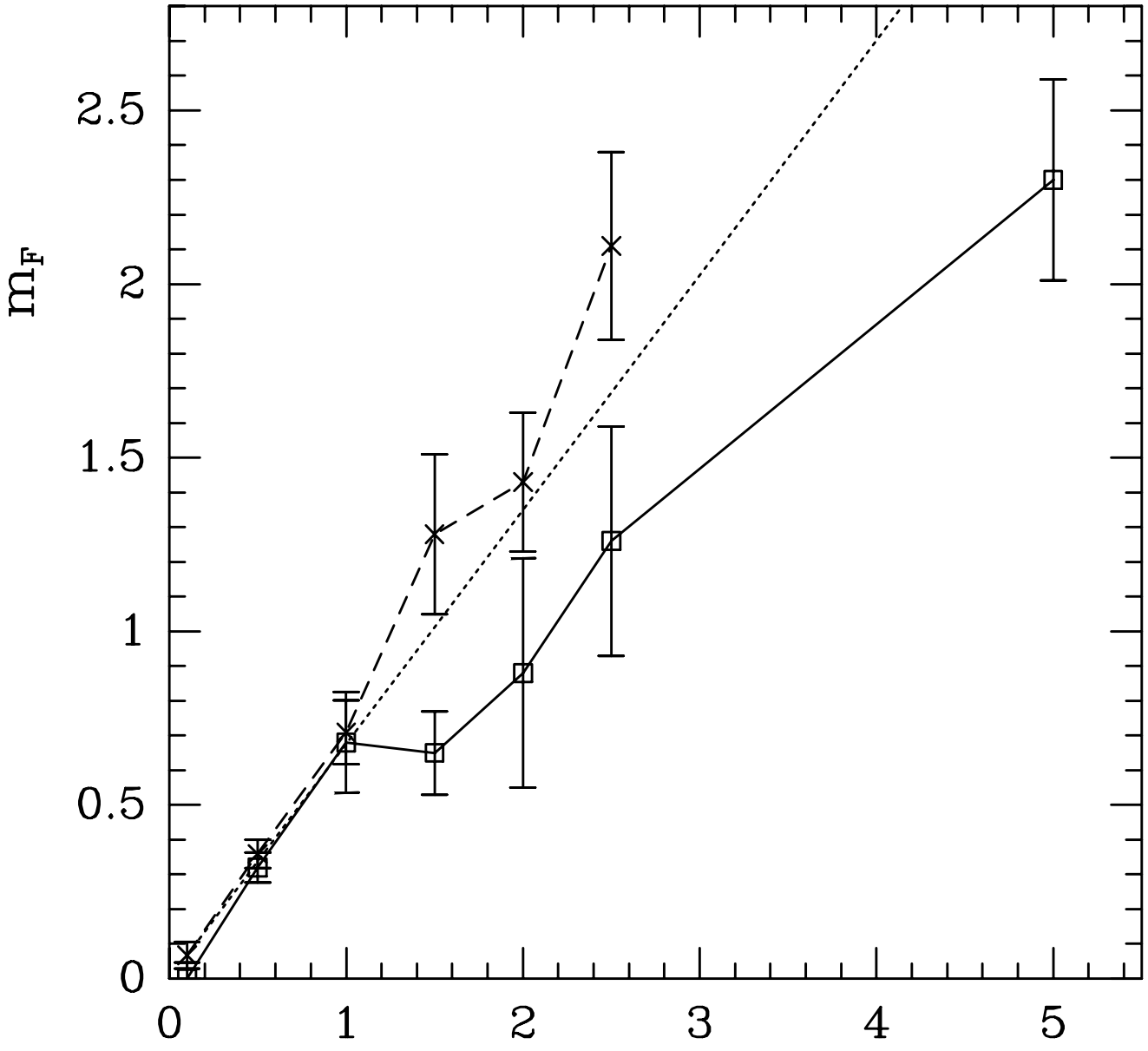

Fig. 7

This figure "fig1-7.png" is available in "png" format from:

http://arXiv.org/ps/hep-lat/9309015v1

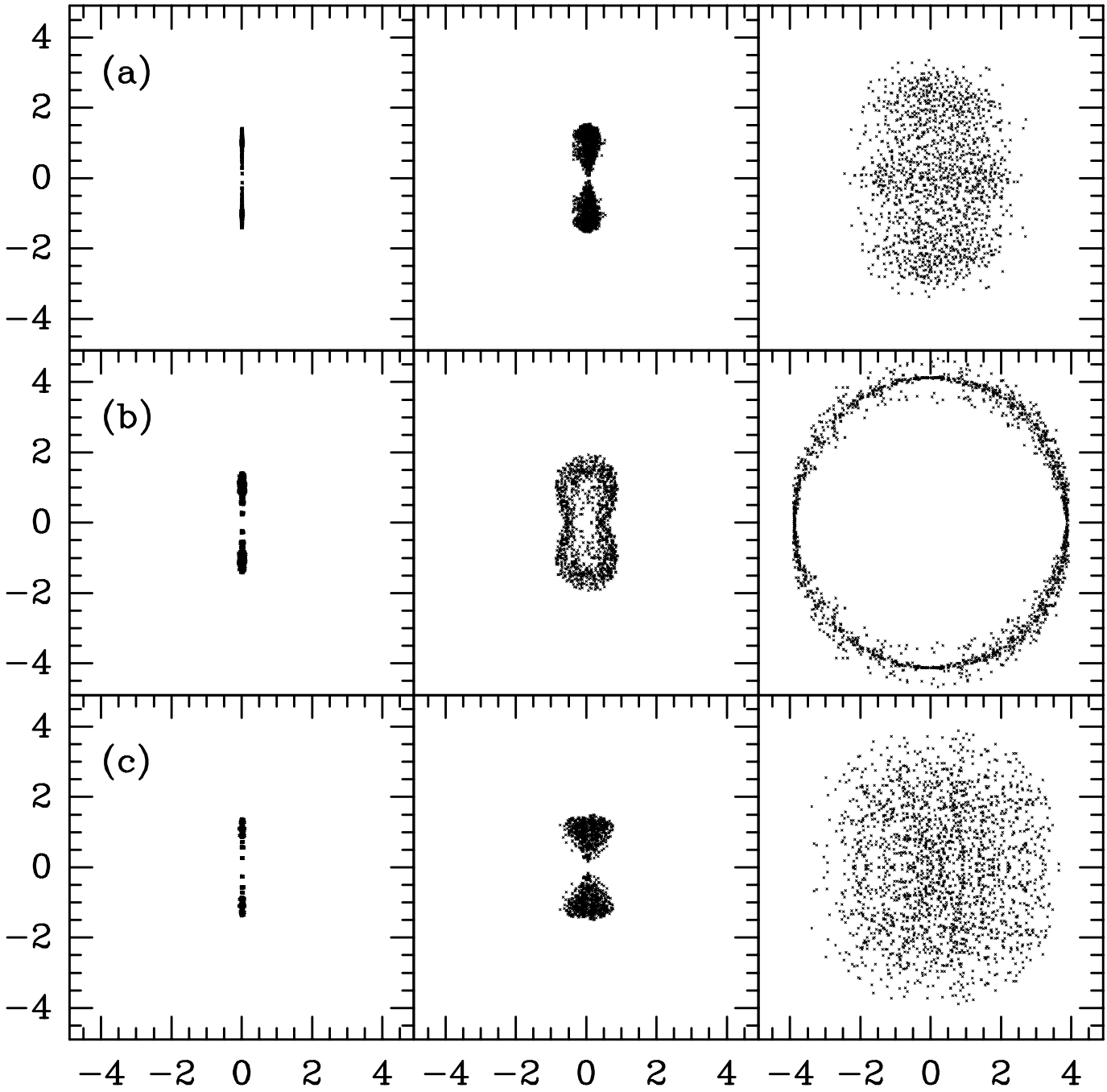

Fig. 8

This figure "fig1-8.png" is available in "png" format from:

http://arXiv.org/ps/hep-lat/9309015v1

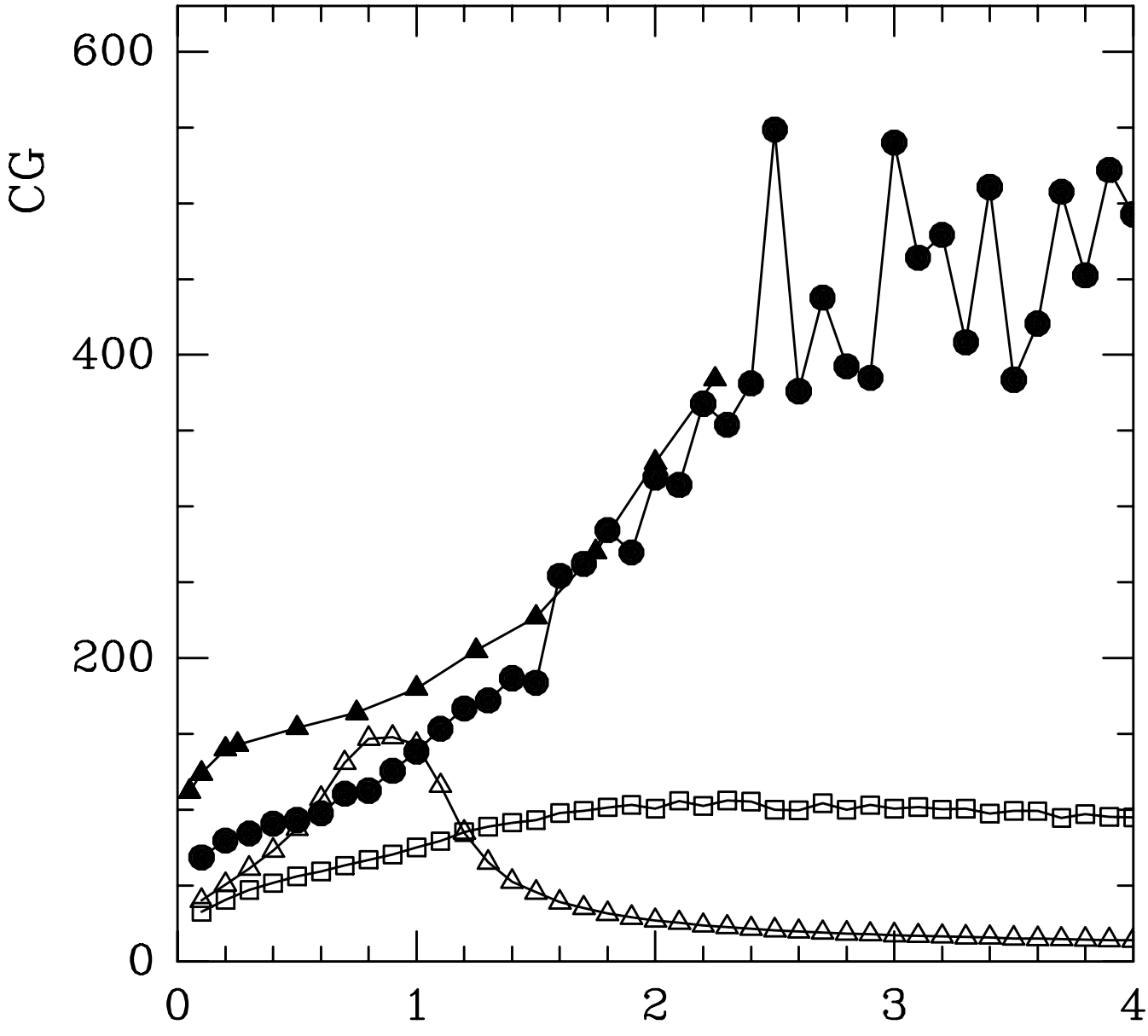

Fig. 9

This figure "fig1-9.png" is available in "png" format from:

http://arXiv.org/ps/hep-lat/9309015v1